

MEMORANDUM AND DEMONSTRATION OFFICE OF THE
SECTION OF SCIENCE (HISTORICAL FACTORS) OF
AMERICAN SCIENCE BOARD

By

CAROLINE ANN GILL HANCOCK

A MEMORANDUM PRESENTED TO THE MEMBERS OF THE
THE UNIVERSITY OF FLORIDA IN PARTIAL FULFILLMENT
OF THE REQUIREMENTS FOR THE DEGREE OF
MASTER OF PHILOSOPHY

UNIVERSITY OF FLORIDA

To Anna Maria, with much love and appreciation

ACKNOWLEDGMENTS

The author would like to express her deep appreciation to the chairman of her committee, Dr. David R. Smith, for his constant guidance, support, and friendship. She would also like to thank her committee members, Drs. Henry C. Mahlich, Arnold R. Hoffman, L. S. Taylor, and Edward P. Smith, for their assistance and suggestions. Thanks are especially given to Dr. Arnold Mahlich for his constant encouragement and personal interest, and Dr. Henry Mahlich for his many hours of patient guidance in teaching the author the techniques of electron microscopy and his continued interest and support of the work. The Department of Biology is thanked for the use of the Biological Electronmicroscopical Laboratory. The author would like to thank Dr. Paul R. Smith, Chairman of the Department of Microbiology and Cell Biology for his interest and help. Special appreciation is given to Dr. Frank R. Basso for his help and for many hours of interesting discussions, and to Dr. Lorraine Wilson for her long hours of diligent help.

The author wishes particularly to express her loving gratitude to her daughter, Anna-Barb, who gave up so much to make this dissertation possible, and her parents, Robert and Mary Galt, for their constant support and encouragement.

This research was supported by the National Science Foundation Grants DE 11204 and DEB 12-24041 and a Grant-in-Aid for Research from Sigma Xi, the Scientific Research Society of North America.

TABLE OF CONTENTS

	Page
ACKNOWLEDGMENTS	111
LIST OF TABLES	iv
LIST OF FIGURES	vi
ABSTRACT	85
INTRODUCTION	1
LITERATURE REVIEW	3
MATERIALS AND METHODS	13
RESULTS	17
DISCUSSION	59
LITERATURE CITED	96
BIBLIOGRAPHIC INDEX	101

LIST OF TABLES

Table		Page
1	Growth of <i>Staphylococcus typhimurium</i> BAC in Yeast Extract- Nutritional Media	18
2	Infection Throat Counts from <i>Staphylococcus typhimurium</i> Inoculated with <i>Staphylococcus typhimurium</i> BAC Harvested from Yeast Extract-Nutritional Media at 24-Hourly Intervals and Stationary Media	21
3	The Effect of Varying the Inoculum Size on Infectious Throat Counts	23
4	Growth of <i>Staphylococcus typhimurium</i> BAC Collected in Soil Extract	25
5	Infection Throat Counts from <i>Staphylococcus typhimurium</i> Inoculated with <i>Staphylococcus typhimurium</i> BAC Harvested from Soil Extract	28
6	Growth of <i>Staphylococcus typhimurium</i> BAC Collected in Corn Meal Medium	31
7	Infection Throat Counts from <i>Staphylococcus typhimurium</i> Inoculated with <i>Staphylococcus typhimurium</i> BAC Harvested from Soil Medium	33

FIGURE

1.	General curves of molecular propagation rate plotted by conventional methods	18
2.	Diagram of interference thread curves of thickness of crystals in the lamellae	20
3.	Carbon-platinum shadowed at $h, h = 1.0 \times 10^{-10}$ m.m. used in the lamellae for the general curve	22
4.	Carbon-platinum shadowed at $h, h = 0.5 \times 10^{-10}$ m.m. used in the lamellae for the general curve	23
5.	Carbon-platinum shadowed at $h, h = 0.5 \times 10^{-10}$ m.m. showing a line of rigid, elastic dense rods	25
6.	Carbon-platinum shadowed at $h, h = 0.5 \times 10^{-10}$ m.m. showing rods of uniform length	26
7.	Carbon-platinum shadowed at $h, h = 0.5 \times 10^{-10}$ m.m. showing symmetrical molecules by which two rods of different lengths have been produced	27
8.	Carbon-platinum shadowed at $h, h = 0.5 \times 10^{-10}$ m.m. showing a line of collapsed rods which are different lengths	28
9.	Carbon-platinum shadowed at $h, h = 0.5 \times 10^{-10}$ m.m. showing a higher magnification of the rods seen in Fig. 8	29
10.	Carbon-platinum shadowed at $h, h = 0.5 \times 10^{-10}$ m.m. showing a line of collapsed rods	30
11.	Carbon-platinum shadowed at $h, h = 0.5 \times 10^{-10}$ m.m. showing rods which are an collapsed along the morphology of the coils as different in diameter	31
12.	A light micrograph of a dense ordered preparation of elementary phase $P = 0.5 \times 10^{-10}$ m.m.	34
13.	Higher ordered preparation of $P = 0.5 \times 10^{-10}$ m.m. showing folded coils	35
14.	A thin section of $P = 0.5 \times 10^{-10}$ m.m. showing electron transparent, full lamellae	36

LIST OF FIGURES--Continued

Figure		Page
15	A thin section of <i>R. trifolia</i> NAG showing an electron dense inclusion	35
16	Effect of suspending <i>R. trifolia</i> NAG in phosphate buffered saline and water	35
17	Growth of <i>R. trifolia</i> NAG in different concentrations of soil extract	37
18	Growth curve of <i>R. trifolia</i> NAG in 48 concentrated soil extract	38
19	Carbon-plasma stained <i>R. trifolia</i> NAG harvested from YEM broth at 12 h	41
20	Carbon-plasma stained 4 h <i>R. trifolia</i> NAG cultured in soil extract	41
21	Carbon-plasma stained 12 h <i>R. trifolia</i> NAG cultured in soil extract	41
22	Carbon-plasma stained 16 h <i>R. trifolia</i> NAG cultured in soil extract	41
23	Carbon-plasma stained 20 h <i>R. trifolia</i> NAG cultured in soil extract	41
24	Carbon-plasma stained 24 h <i>R. trifolia</i> NAG cultured in soil extract	41
25	Carbon-plasma stained 28 h <i>R. trifolia</i> NAG cultured in soil extract	41
26	A light micrograph of a thin section preparation of <i>R. trifolia</i> NAG at 12 h in soil extract	41
27	Growth response of <i>R. trifolia</i> NAG to different concentrations of clover root exudate (pyridine derivat)	44
28	Growth response of <i>R. trifolia</i> NAG to different concentrations of clover root exudate (tryptamine)	47
29	Growth curve of <i>R. trifolia</i> NAG in 50 concentrated clover root exudate	50
30	Growth response of <i>R. trifolia</i> NAG to different concentrations of PEP treated clover root exudate	51
31	Carbon-plasma stained 4 h <i>R. trifolia</i> NAG cultured in root exudate	51

LIST OF FIGURES—Continued

Figure		Page
20	Carbon-platinum electrode 4 h P. <i>trifolius</i> N2O collected in root nodules	37
21	Carbon-platinum electrode 4 h P. <i>trifolius</i> N2O collected in root nodules	37
22	Carbon-platinum electrode 4 h P. <i>trifolius</i> N2O collected in root nodules	37
23	Carbon-platinum electrode 12 h P. <i>trifolius</i> N2O collected in root nodules	37
24	Carbon-platinum electrode 12 h P. <i>trifolius</i> N2O collected in root nodules	38
25	Carbon-platinum electrode 12 h P. <i>trifolius</i> N2O collected in root nodules	38
26	Carbon-platinum electrode 12 h P. <i>trifolius</i> N2O collected in root nodules	38
27	Carbon-platinum electrode 24 h P. <i>trifolius</i> N2O collected in root nodules showing cells of various lengths associated with ethane	38
28	Carbon-platinum electrode 24 h P. <i>trifolius</i> N2O collected in root nodules showing cells of various lengths associated with ethane	38
29	Carbon-platinum electrode 36 h P. <i>trifolius</i> N2O collected in root nodules	39
30	Carbon-platinum electrode 36 h P. <i>trifolius</i> N2O collected in root nodules	39
31	Carbon-platinum electrode 36 h P. <i>trifolius</i> N2O collected in root nodules showing a flow of collapsed cells which are various sizes	39
32	Carbon-platinum electrode 72 h P. <i>trifolius</i> N2O collected in root nodules showing a flow of cells which are various sizes	39
33	Carbon-platinum electrode 72 h P. <i>trifolius</i> N2O collected in root nodules showing a flow of cells which are various sizes	39
34	Mercurially green silver wire with uninfected root hairs	40
35	Short, markedly deflated root hairs (RH) in silver insulated with P. <i>trifolius</i> N2O harvested from the branch at 24 h.	40
36	Long, markedly deflated root hairs on silver insulae harvested with P. <i>trifolius</i> N2O harvested from the branch at 72 h.	40

LIST OF FIGURES—CONTINUED

Figure		Page
44	Tip of spiral root hair when Golgi-stain's secret. Tip on silver is isolated with <i>P. trifolius</i> H&M transposed from 500 levels at 72 to ...	66
45	Inflection turned into root hairs with a shepherd's hook formation.	66
46	Root hair containing an inflection thread which is being lost toward the root section by the root hair nucleus	74
47	Higher magnification of Tip of showing the inflection thread tip and the root hair nucleus	75
48	A thin section of unspunulated bacteria within the silver rhizosphere	75
49	A thin section of an unspunulated bacterium in the silver rhizosphere	75
50	A thin section of unspunulated and partially unspunulated bacteria in the silver rhizosphere	75
51	A thin section of unspunulated and unspunulated bacteria in the silver rhizosphere within a root hair	75
52	A thin section of an unspunulated bacterium embedded in an amorphous material deposited in the root hair cell wall.	75
53	A thin section of spores which contained more than one bacterium	75
54	A root hair with <i>P. trifolius</i> H&M attached in a polar orientation	75
55	An electron micrograph of a thin section of a polarly attached <i>P. trifolius</i> H&M cell	75
56	A diagrammatic illustration of a series of sections over time showing the inflection thread, nucleus, and the formation of walling	78
57	A serial thin section below the inflection thread showing the inflection thread which contained bacteria	78
58	A serial thin section through the walls of the hoop- bacteria showing the inflection thread wall of the root, bacteria within the inflection thread, and the root hair nucleus	78

LIST OF FIGURES-CONTENTS

Figure		Page
41.	A serial thin section past the point the above point out where the wall of the pore is passed by the knife	38
42.	A diagrammatic illustration of a serial sectioned root hair with an infection thread which did not originate in a shepherd's crook	39
43.	The silver wall of the attachment that is passed by the knife in this serial thin section	39
44.	A serial thin section in which the line is continued and the bacteria are revealed inside	39
45.	A serial thin section in which the root hair wall is grazed by the knife	39
46.	A serial thin section showing where the root hair wall is beginning to fragment	39
47.	The root hair is fragmented in front the infection thread in this serial thin section	39
48.	A serial thin section past the middle of the fragmentation	39
49.	A serial thin section in which the back wall of the fragmentation is grazed by the knife, the attached line has ended at this point	39
50.	A thin section of the root hair nucleus which is positioned near to the infection thread	39
51.	A thin section showing the branch point of the infection thread	39
52.	A thin section of an infection thread adjacent to the plant cell nucleus	39
53.	A thin section of an infection thread which gives later the base of the root hair	39

Dissertation Submitted in the Graduate Council
of the University of Florida in Partial Fulfillment of the
Requirements for the Degree of Doctor of Philosophy

PHYSIOLOGICAL AND ULTRASTRUCTURAL ASPECTS OF THE
INFECTION OF CLONED FETAL TISSUE PLACENTAS BY
MYXOMA TRITONII NAOKI

By

Kazuo and Koichi Nagai

August, 1976

Chairman: Dr. David B. McNeill

Major Department: Microbiology and Cell Science

Myxoma tritoni NAOKI was cultured in pure, nutrient-enriched
OEB broth, well screened, and cloned from samples in order to study
morphology and growth characteristics as related to the infection of
clones.

In TEB broth the *Myxoma tritoni* NAOKI had a generation time of 3 h.
Aliquots of cells were taken from TEB broth to determine at what stage
of growth the bacteria were most infective. Inoculum prepared from
stationary phase cells at 15 h gave higher infection thread counts
than inoculum prepared from exponentially growing cells at 15 h or cells
harvested in TEB broth for 30 days. To determine what effect the number
of bacteria in the inoculum had on infection thread counts, 15 h cells
were diluted in serial 10-fold dilutions and used as inocula. 0

100-fold reduction in the number of bacteria in the infection medium is a 100-fold reduction in the infection spread counts, while a 1000-fold reduction resulted in a 100-fold reduction. When standard graphically, the data converted to an exponential increase in the infection threads per seedling with an exponential increase in germination time.

Staphylococcus aureus (SAB) had a germination time of 1.5 h in cold medium. The cells entered stationary phase after 10 h of growth in this medium. Aliquots were taken at intervals from cold medium and bacteria were prepared for infectivity studies. While growing exponentially in cold medium, the cells did not change their infectivity. Bacteria harvested at 14 h and administered produced most infection threads per seedling.

Staphylococcus aureus (SAB) had a germination time of 4 h in sterile seed medium. The cells entered a stationary phase of growth after 12 h of growth in this medium. Aliquots were taken at intervals and prepared as bacteria for infectivity studies. The mean number of infection threads per seedling decreased as the cells aged in seed medium. After 7 days incubation in seed medium, *S. aureus* (SAB) produced 4 times as many infection threads per seedling than did cells incubated for 1 h in seed medium. The measurement of infectivity obtained by seed studies was only consistent with stationary phase cells than with exponentially growing cells.

Electron microscopic examinations of *Staphylococcus aureus* (SAB) *B. trifolii* (SAB) followed the TSB growth, cold medium, and sterile seed medium provided as typical life cycle. Cells followed in each medium had a distinct cell morphology during exponential growth but tended to become more rounded in the stationary phase. Binary fission was the

Each petiole cell distinctly elongated. Asymmetrical cell divisions produced cells of various lengths. Cells cultured in soft agar and those that had been cultured in agar had asymmetrical divisions which resulted in the formation of cords. The occurrence of cords could not be correlated with infectivity. Cells cultured in soft agar became heavily aggregated.

The light and electron microscopes were used to study the physical interactions between host and aphid. The light microscope was used to study the initial invasion of cords, host hair cutting, cell rupture (43). The intensity of host hair cutting could be correlated with the number of virions inoculated into the rhizosphere. With the light microscope it was possible to observe the virions attached to the host hairs in a polar orientation. Infection threads could be observed at low magnification (43). The newly initiated infection thread contacted only slightly with the apices of the host hairs, but became progressively more tight in contact with time. The host hair surface could be observed at the tip of the growing infection thread.

Microstructural studies of several sections of infection threads in cords and hairs showed that the infection thread was initiated by an invagination process. Host hair wall growth was restricted to a localized point, resulting in the formation of an open pore. There was no direct penetration through the wall, and the virions remained encapsulated within the host hair.

INTRODUCTION

The first step in the establishment of the Rhizoctonia-legume N₂-fixing symbiosis is the infection of the host legume by the appropriate Rhizoctonia species. This is a highly specific interaction in which strains of Rhizoctonia are restricted to a particular group of legumes or non-legumes. These restrictions form the basis for speciation in Rhizoctonia and the specialized mycorrhizal groups of host legumes and nonlegumes (Rhizobium).

In the clover symbiosis, infectious strains of Rhizoctonia *trifolii* enter the host through root hairs. The bacteria enter the root host and are enclosed in a cellular structure, the infection thread, which is the first microscopically visible sign of a successful infection.

The physiology of the rhizobia in the soil and the legume rhizosphere is an important consideration in understanding the infection process. The rhizobia are not obligate symbionts but are viable as free living heterotrophs and survive in soil for long periods of time away from the host plant. Little is known of the physiological condition of the cells during this period of resistance in the soil to the stresses of the host, and the possible relation to subsequent infection of an individual host. As the rhizobia come under the influence of the host legume, the bacteria are stimulated to grow and divide. The physiology of the bacteria in root and in culture, prior to and at infection, is unknown.

For this research *R. trifolii* 8436 was cultured in yeast extract-mannitol broth, with nutrient, and clover root nodules to study the growth

of the bacteria as related to the infection of stored under simulated natural conditions. The morphology of the bacteria was followed to determine structurally whether the bacteria passed through distinct morphological changes which would constitute a life cycle as suggested by others in the early 19th century.

The light microscope has been fundamental in studying the growth of the infection spread through the root system. However, the point of entry of the bacteria into the root, and thus the mechanism of infection, cannot be observed with the light microscope. Infections are initiated in slightly curled root hairy tips, in areas where root hairy roots, or in areas covered by bacterial filaments. The electron microscopic examination of electron microtome sections was used as an approach to resolving this problem.

LITERATURE REVIEW

The rhizoids are aerobic, heterotrophic, from negative to 0% O₂ and 9% to 1.5-3.0 pH occurring singly or in pairs, generally germinate young by means of peritheciae, palm, or soft-water filaments. The rhizoids can be effectively classified as "fast growing" or "slow growing" species. Fast growing strains produce acid and have a mean germination time of 2-4 hours. The slow growing strains produce alkali and have a mean germination time of 4-8 hours. Historically, the main taxonomic criterion for including a bacterium in the genus *Rhizobium* is its capacity to form morphologically defined nodules on the roots of a leguminous host. A synthesis between *Rhizobium* and a non-legume, *Frankia*, which resulted in evolution has been reported as an exception to the *Rhizobium-legume* specificity (22).

The rhizoids chemotaxonomically relate normally with the usual *Acidobacteria*. This current working has been attributed to the incorporation of polyphosphatase (23). Craig and Williamson (24) have identified polyphosphate, lipid, and glycogen in bacteroids of *Acidobacteria*. Craig et al. (25) examined bacteroids of 15 strains of rhizoids and found three different inclusion bodies which included polyphosphate, poly-d-hydroxybutyrate, and lipid.

Early workers focused their attention on the phenotypes of the rhizoids and postulated a complex life cycle as suggested by the structure of the host morphology. Beijerinck (26) recognized three distinct types of the rhizoids, aerobic or aerobic nodule bodies,

typical cells, and sometimes in multiple specialized forms. He reported the definitive form of the bacterium to be the medium stained form. Beijerinck (190) observed pure cultures of bacteria in various stages of separation, budding, and branching. He suggested that division occurred as bi-rotation, multi-rotation, and budding and subsequent separation. Lohde and Borch (191) recognized three distinct forms, straight cells, branched cells, and spores. These forms were suggested to exemplify a definite life cycle through which the organism normally passed.

Reiley and Reinholdson (92) found that the lack of available carbohydrates was indicative of a pre-vegetative form, while in the presence of available carbohydrates the cells would develop into a vegetative form and subsequently a seed form. They described a life cycle which they broke down into three stages:

1. The vegetative form (non-viable, small normal). When a nutrient was introduced to a stained cell solution, it was converted after four or five days into the pre-vegetative form.

2. Larger non-viable spores. When pre-vegetatives were transformed to a medium containing carbohydrates, the original stained pre-vegetative increased in size until the spore had formed. At this stage the spores retained non-viability.

3. Spore stage (viable). The cell became elongated and developed high motility. This was recognized as the mature stage of Beijerinck (93).

4. Seed form. The mature proceeded to elongate and develop into a seed form which was still motile, but decreasingly so. As long as there was available carbohydrates, the organism remained in this form.

3. Stage of high concentration. When the organism was placed back into a neutral salt solution for the available carbohydrate was exhausted, it became highly vacuolated and the chromatin divided into a number of bands. Finally these bands became rounded off and merged into the rest of the vacuolated protoplasm.

Thomson and Gangelier (34) followed the changes in morphology of *Shistosoma* and found that a regular cycle of subnormal cells, oval, and band cells successively predominated in soil. The increase in the percentage of oval was associated with increasing bacterial numbers and with the appearance of acidity. The class of appearance of the oval could be controlled by acidification of the culture medium. The addition of milk which 0.2% calcium phosphate would hasten the appearance of the normal form and the movement of the bacteria through the soil.

Gangelier (35) repeated the experiments of Bailey and Hutchinson (4) and confirmed that phosphate hastened the appearance of the mature stage. The bacteria were incubated in soil containing all five stages of Bailey and Hutchinson's life cycle were found. Gangelier found that whether in liquid, agar, or soil, the various life cycle stages occurred simultaneously but in varying proportions. Full metabolites such as urea, creatinine, and presence of certain acids were among the factors that determined which stage predominated.

Various life cycles prepared the isolation of a large "bacterial cell" (which) which was contained a number of mature cells (that) reference, see 35. The organisms were usually released in a succinate condition, and subsequently developed flagella. The term gonitroglyph was proposed by Leitch (that) reference, see 34 for this "bacterial cell" and the organisms were called gonitria. Leitch (36) concluded that the gonitria were (or) the bacterium

and been an indication to reproduction. He could find no regular life cycle correlated with the rhizoids but did observe an orderly sequence in development as cells aged during early and late phases of growth.

Shaw (28) studied the morphology and reproduction of *Blasodinium*. He described such growth forms as rosette, erect, branched forms, gemmule, gemma, and microspore. Reproductive processes consisted of fission, budding, liberation of gemmae, formation of zoosporelike bodies, and germination.

Law (29) studied the growth of the fresh water alga, *Scenedesmus* in various mineral light, fresh nutrient, and soil nutrient and found that the bacteria did not pass through regular stages, although three principal cell types (oval, rhizoided rods, and beaded rods) were observed.

Blount (3,4) suggested a number of stages of *Blasodinium* from a wide variety of plants and observed distinct morphological forms which he regarded as a life cycle. Blount (5) also reported host resistance in some species of *Blasodinium*. Blount and Hale (1) reported that they isolated nematodes from the cell tissue of specialized large hostiles. Graham et al. (30) were unable to demonstrate host resistance when feeding a large number of species of *Blasodinium*.

Went and Warner (31) obtained electron micrographs of *B. rubellum* on the surface of its host *Phallops* which showed structures they interpreted as non-flagellated cilia and multi-flagellated "microvilli". The microvilli ranged in size from 0.1 to 0.3 μ in diameter.

Blount (11) and Hunt (17) have reviewed the survival of rhizoids in soil. In summary, survival in soil is influenced by the plants which have grown there, the physical and chemical properties of the soil, and the stage of *Blasodinium*. The rhizoids can survive in soils in the

abundance of legumes, although numbers are generally higher when the host legume is present. Rhizobium infection was reported to persist for long periods of time in sterilized soil amended with microbial and chemical nutrients with no loss of effectiveness (400). However, Nelson (188) found that *R. trifolii* sporadically produced infection nodules when grown in sterile soil.

Nelson and Beuchamp (175) used gel immobilization to study the persistence of *R. trifolii* introduced into soil by direct root inoculation. They found that bacterial populations of *R. trifolii* diminished with time and confirmed the decrease in competition with naturally occurring rhizobia.

Fluorescent antibody techniques have been used as an approach to the study of *R. japonicum* in the soil (8,126). Free living *R. japonicum* were detected in a variety of soils in the absence of the host legume.

There is a marked stimulation of Rhizobium numbers in rhizospheres, particularly of legumes, when compared with numbers found in soil more distant from the roots. Evidence for both regulatory and inhibitory effects of legume root exudates on Rhizobium has been observed by Khan (11) and Hart (127). Legumes excrete a large number of substances into the rhizosphere, principally sugars, amino acids, and some vitamins (81,185). Legume root exudates stimulate Rhizobium growth (11) but are inhibitory enough to give evidence to account for differences in selectivity. Morgan and Alexander (11) found that a non-invasive strain of *R. trifolii* was a poor root colonizer. Root exudates of Rhizobium root nodules such as Klotz and Schmidt for growth, these are supplied in legume root nodules. Studies have indicated that selection specificity is not determined by selective inhibition (186)

BY JAMES HILL (Ill of Chicago by legume root nodules; different components of the root nodules are stimulatory or inhibitory to the growth of *B. lupinus* (10).

Some legume roots produce a water soluble, thermostable substance that is toxic to varying degrees to Rhizobium strains (11,12). The chemical nature of the toxin is unknown.

Root hairs are the sites of infection by Rhizobium in a large number of legume species, particularly those of the families Fabaceae and Viciae. In the common legume *Aeschynomene eschscholae*, Roberts (13) and we find root hairs and proposed entry of the bacteria through the apical cells. Another important mode of entry of rhizobia is the poles of second root meristems (1,14).

The first anatomically visible perturbation of the host-plant, initiated by infection and swelling of the normally upright root hairs. A characteristic deformation is a swelling of the root hair tip to produce a "shapened's crack" (15). The bacteria enter the root hair and are enclosed in a tubular structure, the infection thread, which is the first visible sign of a successful infection (14). The majority of infected root hairs have the shapened's crack at the infection thread origin, but exceptions exist (11,16). However, not all infected root hairs contain infection threads.

Root hairs of non-legumes are not affected by Rhizobium (16), and studies which tested several species of bacteria indicated that only Rhizobium caused deformation of legume root hairs (16). Root hair deformation is inhibited to some degree by both symbiotic (rhizopod) and non-symbiotic (rhizopod) combinations of Rhizobium and legumes. However, a markedly altered condition of root hairs is almost always

attributed to the lipopolysaccharide associated with definitive rhizobia [11] or their extracellular products [12].

The rhizobial products control plant hormones including indole-3-acetic acid (IAA) and cytokinins (CK). Indole-3-acetic acid (IAA) produced by the nodule bacteria associated by the legume root was thought initially to be responsible for root hair deformation. However, Bellum and Polacco [13] demonstrated that IAA does not, at least alone, cause root hair curling. A strain specific extracellular rhizobial product has been demonstrated to induce root hair curling and deformation [13,14,15,16,17]. Bellum [18] obtained deformities using a host strain preparation obtained by alcohol precipitation. Ljunggren [19] found that rhizobia root hair deforming substances produced by rhizobia in the presence of the host. Bellum and Lee [19] have isolated several deforming substances which contained volatile and non volatile or polymersoluble.

Bradyrhizobium japonicum strains have polymersoluble antigens as their surface which are cross reactive with various antigens on clover roots [20]. Purified preparations of these polymersoluble antigens from infection studies of *B. japonicum* induced lateral root hair deformation on *B. japonicum* *fraxinosa* while polymersoluble antigens from virulent noninfectious isolates produced significantly less deformation than observed on a control weight basis.

Single cells of *Bradyrhizobium* have been observed attached to root hairs and epidermal cells in a polar (end-on) orientation [21,22,23,24,25,26]. Polar attachment is not restricted to the *Bradyrhizobium-lupinus* symbiosis and has been observed with bacteria attached to the epidermal surface in germinating roots of other [21]. *Plasmodium* and *Sphaeromonas*

show polar orientation of cell wall and cellulose synthesis (23) is there some polar organization could not be explained by localization of surface isotropic groups.

The molecular basis for polar orientation of fibrous cells is unknown. Ishida and Ishida (19) suggested that specific interactions between cellulose and the two halves of the host layers may involve binding between lignan residues and the bacteria. Ishida and Ishida (19) have demonstrated that *Tricorynus flavescens* uniformly in *E. japonicus* host root locally at one end of the cell. *Tricorynus flavescens* isolated culture media was also observed to bind preferentially at cell poles. The authors pointed out that it remained to be determined if polar matrix binding and polar synthesis occur at the same end of the cell. Stone and Ishida (18) have proposed a model whereby specificity in the *E. trifida*-derived symbiosis is based on interactions of some residual surface epitopes that are cross bridged by a multivalent alien matrix.

Several theories have been proposed regarding the entry of the bacteria into the root hair. Hansen (24) has advanced the hypothesis of root hair wall invagination. An invagination results from the inflexion of plant cell wall growth as a localized pole, resulting in the wall growing back into the root hair to form the tubular inflexion region. There is no penetration through the wall at the point of entry, and the bacteria remain extracellular, i.e., there is no direct contact with the host cytoplasm.

Hansen's theory of invagination has been challenged as several points. First, how the wall wall invagination specifies the high specificity present at the root hair is unknown (11). Secondly, invagination

would form an open pore, which had not been shown in earlier electron micrographs (23,24). However, serial sections of root hairs were not used in these studies. Additionally, an open pore would allow simultaneous entry of different wall types which would result in the presence of several *Shiobolus* strains in a single subunit. Early studies believed that only one strain of *Shiobolus* was isolated from a subunit when the hair had been inoculated with a mixture of infective strains differentially marked by antibiotic resistance (25) or serological type (21,42). However, recent studies (21,44) have shown that several strains can be isolated from one subunit.

Kjansson and Polman (41) have proposed a "polyphenolomannan" hypothesis in which the cellulose-mannopolysaccharide interface plant cells mayes collectively and a single bacterial cell surface and subsequently penetrates the plant cell wall without provoking structural disruption. The infection threat is presumably reduced once the bacterium penetrates to the plant plasmalemma.

In support of this theory these workers demonstrated that a crude preparation of microbially polysaccharide of *Callosium rhodii* decreased the viridity or *de novo* synthesis of plant produced penicillins against. This viridity was strain specific in that it correlated with the plant-bacterium specificity. Mann (44) provided evidence to support this theory and demonstrated that the isolation of penicillin (penicillin transublimation) was acid sensitive. Indeed (43) found penicillins unique activity was not correlated with infectivity of virulence. In addition, other workers (45,51,54) have not been able to verify this hypothesis.

The microbially polysaccharide of *Shiobolus* has been well characterized in some cases. Upper (43) found glucose, galactose,

glucuronic acid, pyruvic, and succinic in extracts of *B. trefolex*. Small differences in composition between strains were not related to the ability to nodulate or to the capacity of the symbiotic organism to fix nitrogen. Bunt (17) examined extracellular polysaccharides from *B. meliloti*, *B. trefolex*, *B. pascuensis*, and *B. lupulinae* and could find no significant differences in carbohydrate composition with the exception of *B. meliloti*, which lacked succinic acid. Polysialic acid was a common constituent of *B. lupulinae*, *B. trefolex*, and *B. pascuensis* (24,25,26). Cellulose has been identified in all the fast-growing strains as well as pyruvic and succinic acid (26,24). Cellulose has been identified as an extracellular product of some strains of *Brassicella* (26,26).

Bunt (22) examined strains of *B. trefolex*, *B. lupulinae*, *B. japonica*, and *B. pascuensis* and found both capsulated and bare cells, with the latter predominating. Otsu and Ishikawa (23) reported capsule formation in a strain of *B. trefolex*. This capsule was characterized as a high molecular weight ($> 4.5 \times 10^6$ daltons), β -linked, acidic heteropolysaccharide consisting of D-glucuronic, galactonic, glucosic, and glucuronic acid.

For various fast-attained ultrastructural studies of infected root hairs. Bunt and Peterson (24) and Sigwalt (25) examined infected clover root hairs under the electron microscope. These authors did not section infected root hairs through the origin of the infection. Bunt and Sigwalt offer phase micrographs in support of Bunt's theory of invagination (26). Hart (26) examined root hairs under the scanning electron microscope. He reported that root hairs and epidermal cells were coated with many bacteria, some of which appeared to be embedded in the wall. The root hair tips were often smooth but some older root hair surfaces had a fibrillar network pattern.

MATERIALS AND METHODS

Anterior stream--dendrotoxic *Trichos* milk, indigenous to *Th. pallens* *fragiformis* was obtained from W. F. Hudson.

Media--Aerobically supported medium (YEM) broth (18) was prepared, stored for 15 min, filtered through Whatman No. 1 6294A paper to remove excess CaCl_2 , and sterilized by autoclaving.

Well nutrient was prepared by standing 1 kg air dried soil (2 541 medium content) with 1 liter deionized water for 30 min. The nutrient was centrifuged at 15,000 x g for 10 min to remove soil particles, filtered sequentially through 5 μ m and 0.45 μ m membrane filters (Gibco Laminated Co., New Haven, Conn.), lyophilized and stored deaerated. The dry weight of soil nutrient as prepared from 1 kg of soil in a liter of water was 440 mg/l. Deaerated soil nutrient was filter sterilized by passage through a 0.2 μ m membrane filter.

Seed media was prepared from *T. fragiformis* var. *fulvipes*. The seeds were surface sterilized with 5% HgCl₂ for 10 min and flamed successively with sterile deionized water. The seeds were dispersed in peptone water containing mixed H₂ water agar (sterilized agar, Miles Laboratories, Kalamazoo, Mich.) impregnated at 10%, and the agar allowed to harden. The agar-seed slabs were transferred to sterile storage dishes (Corning No. 208, 120 x 90 mm) which contained stainless steel mesh holders (14 mesh stainless steel wire cloth, Smith Parts Inc., Miami, Fla.) to position the slabs above but not touching the water. The media penetrated through the stainless steel into 70 ml of sterile

delimited using [4] [3,8]. The root nodules were harvested after 7 days. Filament continuously through 1 µm and 0.45 µm membrane filters, lyophilized, and dried desiccant. Glens root nodules are prepared had 100 µg dry weight/ml water. Sterilized root nodules was sterilized by passage through 0.2 µm membrane filters.

Growth Conditions--Inocula were inoculated in a rotary shaker (400 rpm) maintained at 25 °C. Growth curves were determined by growing 2 deliquescent 30/30 in appropriate media in aseptic culture flasks (Bellco Glass Inc., Vineland, N. J.) and measuring the optical density in a Bausch and Lomb Spectrophotometer 20.

Harvesting--Bacterial trifolium 30/30 was grown in 500 broth and harvested in mid-exponential phase (12 h). Cells were centrifuged from YEM broth at 11,200 x g for 30 min in sterile 50 ml centrifuge tubes and washed twice in filter sterilized phosphate buffered saline (PBC: 0.05 M Na_2HPO_4 - KH_2PO_4 , 0.15 M NaCl , pH 7.0).

Dry Weight Determinations--Cell mass determinations were made by filtering 10 ml samples through 0.45 µm bacteriophage filters (Chesapeake Corp., Piquette, Pa.) The filters were dried at 60 °C for 30 min, cooled for 5 min, and weighed. This procedure was repeated at least twice to insure a stable weight. After cooling, the process was repeated to determine the weight of the inocula.

Dry weight determinations of soil extracts and root nodules were made by lyophilizing 5 ml of extract in acid cleaned, pre-weighed ampules. All samples were done in triplicate.

Bacterial-Plant Interactions--*Bradyrhizobium japonicum* var. *sojae* infection seeds were surface sterilized, rinsed and acid treated for 48 h at 4 °C (8,1). Seeds were germinated overnight (darkness under agar plates)

cells until all at 22 °C and transferred to Polysar glass-walled assemblies (15) inoculated with appropriate cultures. The assemblies were incubated in a plant growth chamber (Growth Room, Model GH-150-S, Newhall, Calif.) programmed at 22 °C (darkness), 12 h photoperiod, 2000 lux light intensity (approximately 20000-25000 erg/cm²/sec) and 60% RH, using growth in 1000 hours (400), protoplast cellulose sclerotization which resulted in filamentation. Fibers were usually observed and counted from 1 to 3 cells. Isomers were prepared for infectivity studies by centrifuging E. coli (10) 5000 g for 10 min in sterile bags 10 ml centrifuge tubes at 11,000 x g for 10 min. This treatment determined by use of a Beckman-Bioscan bactericidal counter. Isomers were standardized with appropriate volumes of Polysar assembled 100, *Tricholium* /*Tricholium* var. *Tricholium* assemblies were inoculated and infectivity titrations measured after 3 days (infectious titer using phase contrast microscopy).

Electron Microscopy Studies—Equal volumes of 40 glycerol/oligo and isomers (in oligo solution were mixed together. The bacteria were fixed for 1 h and washed successively with PBS and distilled water. Cells were stuck on 200 mesh formvar-coated grids and stained at approximately 45 degrees with uranyl and platinum in a Balzers MB3000 freeze-etch apparatus (Balzers, Inc., Friesenheim, Switzerland).

For negative stained preparations, bacteria were centrifuged from PBS broth at 11,000 x g for 10 min and washed successively with PBS and distilled water. A drop of bacteria and a drop of 2% phosphotungstic acid (pH 7.0) were placed on a 100 mesh formvar-coated grid and allowed to set for 2 min. The excess liquid was drained from the grid and the grid was allowed to dry.

Three and 7 day old viable glass assemblies from Polysar assemblies

were fixed at 22 °C for 1.5 h with 1.5M cacodylate buffer, pH 7.4, and post-fixed at 22 °C for 1.5 h with 1% tetrarad sodium osmium. Samples were dehydrated through a graded ethanol series (25, 50, 75, 91, and 100%). The 75% ethanol contained 1% uranyl acetate. Sections followed the ethanol series and the tissue was infiltrated with liquid resin (10) and polymerized overnight at 60 °C. The sections were flat embedded in epon-epoxy. Post-embedding disposable embedding media (EM-6000; Post-embedding Sectioning, South EL Science, Inc.). The embedded sections were cleared with glass mounted microscopy, and some containing inclusion threads were selected for sectioning. Serial sections were cut on a Sorvall MT8 Ultratome with a diamond knife. The sections were picked up on deionized water nit-hole grids and stained with Reynolds' lead citrate (14).

Sections were prepared for thin sectioning using the same procedure. The cells were embedded in 1.0% agar above post-fixation with 1% osmium tetroxide. The agar was not left small blocks (2-3 mm cubic) and the dehydration and infiltration with plastic continued.

Carbon-platinum shadowed grids, negative stained bacteria, and grids containing thin sections were examined in a Zeiss 10A electron microscope operating at 15 kV.

RESULTS

Growth of *Blaschkea tripartita* B&P in Tissue Culture-Medium (TCM) broth is a standard laboratory method used for the culture of *Blaschkea*. It was selected for use in this study because it is a complex growth medium in which variations would be in nature. Different morphological forms of *B. tripartita* B&P, if found during growth in this medium, would be characteristic of a more physiologic nature and not artifacts induced by culture conditions.

A growth curve (Fig. 2) was determined for *B. tripartita* B&P in TCM. It would be known when the cells were actively growing (exponential growth) and in a stationary phase. *Blaschkea tripartita* B&P had a maximum generation time of 1 h in TCM broth. Fig. 1 shows that a 48 h incubation had essentially no lag period when transferred to new medium. Cells were at exponential phase in 20-12 h and in stationary phase at 14 h. As seen in Table 1, the pH of the medium became slightly acidic during the growth of the bacteria.

Blaschkea tripartita TCM produced colonies characteristic but not identical during all phases of growth in TCM broth. The cells were evenly dispersed and contained from 1 to 4 cells. Aliquots of cells were taken from TCM broth at 12 h, 17 h, and 28 days and prepared as inocula for infectivity studies. Infectious was defined as the ability to induce an infection shown in clover root lesions. Inocula per milliliter were standardized to 10^6 cells/ml.

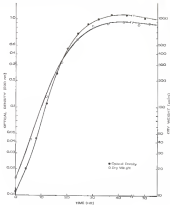


Fig. 1. Growth curves of *Rhodospirillum rubrum* R20 cultured in photo-microaerobic liquid.

Table 1 Growth of *Monodon* trophus B66 in Fresh Seawater-Nutrient Media

Time of Incubation (hr)	Optical Density 420 m μ	Growth Phase	pH of Medium
0	0.1	Incubation	7.8
4	0.30	Early Exponential	7.1
11	1.00	Mid-exponential	6.8
18	2.01	Late Exponential	6.8
24	7.00	Early Stationary	6.4
30	6.00	Stationary	6.4
36	6.00	Stationary	6.5

Table 3 gives infection threat counts after 3 days for the different ages of larvae. Larvae prepared from stationary phase cells at 72 h gave the highest infection threat counts (Table 3). As indicated by the high standard deviations for 72 h and 75 days, infection threat counts tended to be variable from one sampling to another for a given inoculum. This variability could perhaps be reduced somewhat by using an infected variety of chicken.

An analysis of the variance indicated that the mean number of infection threat counts for 72 h cells was significantly higher than for the other two cell ages at the 5% level of confidence. Larvae prepared from 72 h stationary phase cells were more infectious than larvae prepared from 36 h or 75 day old cells. Infection threats were significantly higher at 36 and 42 h after inoculation of the suckling. This infection then remained constant and did not vary with the age of the inoculum. There is, then, at least a 36 h period of time when the bacteria may come under the influence of the host. Cells at 72 h stationary phase were able to establish a more efficient bacteremia which led to infection.

Bone hair absorption was measured to determine if the age of the follicle affected bacterial attachment. Bacterial suspension consisting of single cells, as opposed to flocculated cells, were prepared by filtering cells through glass wool. Cover slottings were set up in laboratory glass slide apparatus (21) and inoculated with single cells prepared from 36 h and 72 h B. anthracis 8829 cultures in YEM broth. There was no detectable difference in bone hair absorption between 36 h and 72 h cells (4 ± 2) and $4 \pm 2-3$ bacteria/cm² hair, respectively. The slottings were examined after 36 h inoculation in the dark. Bacterial attachment for 75 day old cells was not examined.

Table 2 *Delphinids and Calves from the Pacific Ocean Interpreted as a Population Originated from Point Lascruces—Prenatal Death and Abnormalities and Abnormalities at Birth*

Total No.	Age at Interval		
	12 hr.	32 hr.	78 days
1	10	145	20
2	14	45	40
3	26	112	34
4	26	40	41
5	15	112	24
6	14	91	41
Total	76 \pm 4.61	458 \pm 29.3	109 \pm 13.4

There were no detectable differences in root hair deformation or swellings associated with 2.5 h and 72 h coils. Both preparations had markedly deformed root hairs which were shorter than uncoiled controls. These deformed root hairs ranged from 8.5% to 0.3 μ m. The swellings associated with 72 day old coils had longer root hairs than did uncoiled controls (greater than 2.5 μ m).

To determine what effect the number of bacteria in the inoculum had on infection thread counts, 72 h coils were diluted to serial 10-fold dilutions and used as inocula. Table 3 gives the infection thread counts after 3 days. An analysis of the variance was performed on the infection thread counts given in Table 3. An *F* test indicated that, at the 5% level of confidence, there was a significant difference in the mean number of infection threads among the different sizes of inocula.

The mean number of infection threads was the same for the seedlings inoculated with 1.1×10^8 and 1.7×10^7 bacteria; however, the standard deviation for the latter was larger indicating a greater variance among counts. This inoculum (1.7×10^7) was able to induce 72 infection threads on one of the seedlings, which was a higher count than observed on any seedling inoculated with 1.1×10^8 bacteria. The inoculum prepared from 1.1×10^8 bacteria also gave a high count of 31 infection threads on one of the seedlings, but again there was a large variance in counts. This inoculum had a lower mean and a higher standard deviation than did the first two inocula.

A 100-fold dilution in the number of bacteria in the inoculum resulted in a 55% reduction in the infection thread counts, while a 2000-fold dilution resulted in a 55% reduction. When examined graphically (Fig. 11), the data indicated an exponential decrease in the infection

Table 2 The Effect of Varying the Injection Rate on Injection Thread Counts

Trial	Pressure (psi)			
	2.3×10^3	3.3×10^3	4.3×10^3	5.3×10^3
1	47	77	26	54
2	44	58	52	21
3	47	31	21	24
4	52	48	21	21
5	56	26	24	21
6	54	20	17	17
Mean	50 ± 4.4	34 ± 14	20 ± 11	24 ± 4.8

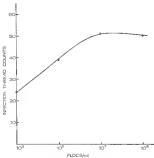


Fig. 2. Relation of Infection Threshold Counts to the value of Inocula in the Lactolysis.

thoroughly well, resulting with an exponential increase in the bacterial mass, up to 10^8 (bacteria), at which point a plateau was reached.

Morphology of *Shewanella belfragei* DSM in Fluid Nutrient-Mediums
 broth.—The morphology of *S. belfragei* DSM was monitored by examining the cells under the light microscope using the standard Gram's stain and the electron microscope using carbon-platinum-coated preparations.

Shewanella belfragei DSM had two types of envelopes, poly- α -hydroxyphosphoglycans (PHG) and dark, polar inclusions which resembled polyphosphate bodies characterized in other bacteria by Dalg and Williamson (15) and Dalg et al. (24). PHG was not apparent in carbon-platinum stained cells but could be seen in iron-sulfide preparations as non-existing areas. Polar bodies could be seen in carbon-platinum stained preparations when the bacteria were collapsed. If cells were not collapsed, they were too electron dense to discern polar bodies. Polar bodies could be seen occasionally in thin section preparations as thin polar inclusions within a thin negative cell. The frequency of the blue color was variable among preparations which may have been a reflection of the extent of alcohol washing.

The representative morphology of the 41 h bacteria used for the growth curve in Fig. 1 is shown in Fig. 3 and 4. The predominant form of the bacteria at this time was a rod. Pairs of cells were associated with cellulosic microfibrils as indicated in Fig. 3. The bacterial cells were collapsed and the electron dense polar bodies could be seen (Fig. 4). The length of the rods was variable and this variability was attributed to slightly asynchronized cell divisions as seen in Fig. 4.

When starting the culture at this time showed a homogeneous population of short, rounded rods. The cells were filled almost entirely with

Fig. 1. Carbon-platinum shadowed at 1.5×10^5 v/cm; 0.001 sec, used as the basis for the growth curve. This micrograph shows a film of rods with collinear microfibrils (CMF). The rods are of various lengths. (X 1,800)

Fig. 4. Carbon-platinum shadowed at 1.5×10^5 v/cm; 0.020 sec, used as the basis for the growth curve. This micrograph shows a film of rods which are of various lengths. The more lateral end of division indicates here an asymmetrical division has produced a short and a long rod. CMF indicates collinear microfibrils. (X 11,100)

Fig. 5. Carbon-platinum shadowed at 1.5×10^5 v/cm; 0.040 sec, showing a film of rigid, electron dense rods. Collinear microfibrils (CMF) are associated with the rods. The film is composed of rods of various lengths. (X 1,800)

Fig. 6. Carbon-platinum shadowed at 1.5×10^5 v/cm; 0.060 sec, showing rods of uniform length. CMF indicates collinear microfibrils and CM indicates cross fibrils. (X 4,800)

Fig. 7. Carbon-platinum shadowed at 1.5×10^5 v/cm; 0.100 sec, showing an asymmetrical division by which two rods of different lengths have been produced. (X 11,100)



PHB as that only the poles of the cells were stained. Some cells stained in a beaded pattern which was attributed to the accumulation of PHB. Polar bodies were not seen in the first stained preparation.

Shewanella putrefaciens 8420 was in early exponential growth 8 h after inoculation into YEM broth. The representative morphology of the cells at this time is shown in Fig. 1. The cells appeared more rigid at 8 h and were less electron dense in one polar body. The length of the rods was variable, and were limited to roughly spherical and to short short elliptical and hexagonal. Some stained preparations at this time showed the cells were less vacuolated than the incubation, but the cells continued to appear beaded.

Fig. 2 shows representative morphology of *S. putrefaciens* 8420 at 11 h, which was mid-exponential growth. There was little difference in the morphology at this time when compared with cells at 8 h. The cells continued to appear rigid and cationic microfilaments were absent upon high doses of tetracycline. At this time the length of the rods was the same uniform during growth in YEM broth. Some staining of the cells at 11 h showed less vacuolation than at 8 h, but the staining of the cells appeared slightly beaded.

At 18 h *S. putrefaciens* 8420 was in late exponential growth in YEM broth. Fig. 3 shows a stained preparation of cells at this stage. The cells were less electron dense, which indicated collapse. The cells were rigid during exponential growth, but collapsed when in or approaching the stationary phase. When cells collapsed, it was possible to see the polar bodies. While the cells were still distinctly rod shaped at 18 h, a tendency toward shorter rods was apparent. Some stained preparations of 18 h cells showed a slight increase in vacuolation.

The morphology of the cells at this stage was distinctly rod shaped when viewed under the light microscope.

After 18 h *P. troglodytes* BMD entered stationary phase. As seen in Fig. 8-12, as the cells aged in T81 broth, there was a tendency to become rounded and progressively more collapsed. Fig. 9 is a low magnification of a film of 20 h cells shown collimated microscopically. A higher magnification of the cells showing more detail of the collimated microscopically and a polar body is shown in Fig. 9. In most cases, the collimated microscopically appeared as if compressed in the plane of the slide, but sometimes did not. Fig. 10 and 11 show cells at 30 h and 40 h, respectively. As cells aged, the amount of collimated microscopically appeared to decrease. At 44 h (Fig. 12) the cells were quite collapsed, even more so than the original 18 h inoculum (Fig. 8).

Two marked properties of stationary phase cells were consistent in that the cells became highly vacuolated and staining was restricted to the poles of the cells. At 40 h, some marked properties had distinct polar bodies within the cells. Fig. 13 shows a light micrograph of a low magnification preparation of *P. troglodytes* BMD. The narrow indicates the polar bodies which give the rods a limited appearance. The clear, vacuolated areas within the cells are attributed to the stimulation of PH.

The limited appearance of the cells was also seen under the electron microscope with negative stained bacteria. Fig. 14 shows 40 h *P. troglodytes* BMD with a limited appearance due to the middle of the cytoplasm being electron transparent and the poles of the cells being electron dense. Within the electron transparent middle region were very small, spherical, more electron transparent inclusions.

Fig. 8. Cryoelectron shadowed M & P. *trichia* 8428 showing a ring of collapsed cells which are different lengths. DB indicates a long bundle of cellulose microfibrils. (X 54,000)

Fig. 9. Cryoelectron shadowed M & P. *trichia* 8428 showing a higher magnification of the cells seen in Fig. 8. The arrow indicates a bundle of cellulose microfibrils (DB) at the pole of the cell. PE indicates a polar body in a short, rounded cell. (X 64,000)

Fig. 10. Cryoelectron shadowed M & P. *trichia* 8428 showing a ring of collapsed cells. (X 10,000)

Fig. 11. Cryoelectron shadowed M & P. *trichia* 8428 showing cells which are so collapsed that the morphology of the cells is difficult to discern. (X 10,000)

Fig. 12. A light micrograph of a thin section preparation of embryonic phase *P. trichia* 8428. The arrows indicate the dark staining polar bodies which give the cells a beaded appearance. (X 4,000)



8



9



10



11



12

13

Fig. 12. Negative electron projection of P_{-} (solid) and P_{+} (dashed) inside coil (X 10,000)

Fig. 14. A spin section of P_{-} (solid) and P_{+} (dashed) showing electron consequent PMS interaction (X 10,000)

Fig. 15. A spin section of P_{-} (solid) and P_{+} (dashed) showing an electron source location (X 10,000)

13



14



15



In this section (Fig. 14 and 15) these incubations were with an small and diffuse or no larger electron transparent areas with no evidence surrounding them. The electron dense inclusions were also not surrounded by membrane, however, Fig. 15 shows evidence within the cytoplasm. Fig. 14 and 15 were 42 h, exponentially growing cells.

Forming mid-exponential cells--Shewanella trophica RAB cells were harvested from FBR broth at 12 h by transfer to well mixed and sterile water media. Cells at 12 h (mid-exponential growth) were placed in Shewanella slant, at this time, the cells had a uniform cell morphology (see Fig. 9 and 10). The purpose of these experiments was to show whether or not well mixed or poor medium could induce *S. trophica* RAB to undergo morphological changes which could be considered as constituting a life cycle.

Fig. 16 shows the effect of harvesting and resuspending cells in phosphate buffered saline (PBS, pH 7.2) or distilled water (D₂O). The optical density and dry weight of the cells was monitored for 5 h. The optical density of the cells resuspended cells decreased while the optical density of the FBR resuspended cells remained fairly constant. Phase and microscope examination showed that flocculation was not caused by resuspending the cells in water. The decrease in optical density was attributed to flocculation. When FBR and water resuspensions were examined on a dry weight basis, both decreased 10 times at the same rate (Fig. 16). It was decided to use FBR as harvest and resuspend *S. trophica* RAB in order to avoid excessive flocculation.

Growth of Shewanella trophica RAB on Solid Medium--The dry weight of well mixed as prepared from 1 kg of soil in 1 liter of water was 440 mg/ml. This concentration of well mixed was called 1% Soil.

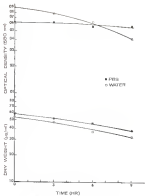


Fig. 34. Effect of succinyl chondroitin disulfate (SCD) in phosphate buffered saline and water.

extract could not be concentrated further than 5 times when using lyophilized soil extract. The dry material could not be completely resuspended. The following concentrations of soil extract were prepared: 1.0E (4400 mg/ml), 1.0E (2200 mg/ml), and 4E (1170 mg/ml). *S. aureus* 8320 was harvested from TSB broth at 18 h (mid-exponential growth) and resuspended in the different concentrations of soil extract. The growth of the bacteria was monitored by optical density. As seen in Fig. 37, the usual growth of the bacteria, rather than the protection time, was affected by the different concentrations of soil extract.

Staphylococcus aureus 8320 was harvested from TSB broth at 12 h and resuspended in 4E concentrated soil extract. The growth curve is shown in Fig. 38. The same protection time of the bacteria in 4E soil extract was 3.5 h. By the time the cells entered stationary phase (Fig. 4), the cell mass had approximately tripled. As indicated in Table 4, the pH of the culture increased during the growth of the bacteria in soil extract. The cells neither produced alkaline end products nor consumed an acidic substrate. There was no buffer added to the medium.

Samples of cells were taken from soil extract at intervals and prepared as inocula for infectivity studies. Total cell counts in the inocula were standardized to 10^8 cells/ml. Table 5 gives infection phage results after 5 days incubation. While the cells were growing exponentially (up to 22 h) in soil extract, the cells did not change their infectivity. Cells from stationary phase (at 24 h and thereafter) failed to infect phage through per inoculum. Due to the presence of noninfectious flora, the viability of the cultures could not be accurately determined. Infection through per inoculum was initiated within the time range of 28 to 42 h after inoculation. This time range did not vary with the age of the inoculum.

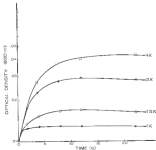


Fig. 17 Growth of *Rhodospirillum rubrum* in different concentrations of cell extract.

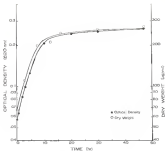


Fig. 12 Growth curve of *Brucella* (v/v) 8230 in 4% concentrated cell extract

Table 4. Growth of *Neisseria meningitidis* 8000 cultured in DMEM medium

Time of Incubation (hr)	Optical Density 630 nm	Growth Phase	pH of Medium
0	0.00	Sequelant ion	7.4
1	0.04	Mid-exponential	7.3
10	0.214	Early Stationary	7.4
24	0.40	Stationary	6.8
48	0.215	Stationary	6.8

TABLE 1. *Summary of the results of the analysis of variance for the effect of the treatment on the response of the subjects to the treatment.*

Treatment	No. of subjects	Analysis of variance				Analysis of variance			
		df	SS	MS	F	df	SS	MS	F
1	10	9	1.14	.127	1.14	9	1.14	.127	1.14
2	10	9	1.14	.127	1.14	9	1.14	.127	1.14
3	10	9	1.14	.127	1.14	9	1.14	.127	1.14
4	10	9	1.14	.127	1.14	9	1.14	.127	1.14
5	10	9	1.14	.127	1.14	9	1.14	.127	1.14
6	10	9	1.14	.127	1.14	9	1.14	.127	1.14
7	10	9	1.14	.127	1.14	9	1.14	.127	1.14
8	10	9	1.14	.127	1.14	9	1.14	.127	1.14
9	10	9	1.14	.127	1.14	9	1.14	.127	1.14
10	10	9	1.14	.127	1.14	9	1.14	.127	1.14

NOTE: df = degrees of freedom; SS = sum of squares; MS = mean square; F = F-ratio.

Morphology of *A. baumannii* in CF sputa that is shed (green)—All parts were taken at intervals to determine if *A. baumannii* B20 passed through distinct morphological changes which could be called a life cycle as proposed by another author (1,2,13,18,19)

Fig. 18 shows the representative morphology of *A. baumannii* B20 harvested from TB broth at 21 h. Cells at mid-exponential growth were fairly uniform in morphology. At that time most cell divisions were equatorial so cells were of a uniform length. Cells at this stage of growth were too distinct from *S. aureus* to see polar bodies.

The representative morphology of *A. baumannii* B20 cultured in cell extract (48, concentrated) is shown in Fig. 19-21. Throughout growth in cell extract, the predominant morphological form of the bacteria was a rod. The rods remained rigid through 16 h (Fig. 19-20) but at 21 h (Fig. 21) the cells appeared collapsed.

Asymmetrical cell divisions resulting in the formation of short biased segments at 6 h (Fig. 19). At this time approximately 11 of the rods had a narrow focusing at the pole of the rod. The rods were the same diameter as the rod. Formation of short continued through the 11 h sampling (Fig. 21) and 14 h sampling (Fig. 22). At 14 h the frequency of occurrence of short at the poles had decreased to 11 of the rods. In one cell about 16 h (Fig. 23) that two short were detected in the rod. At this time two rods in the medium resembled approximately 11 of the rods.

At the 11 h sampling (Fig. 23), the rods were collapsed. While morphology became somewhat distorted due to collapsing, the variability in rod length could be detected and short were seen at the poles of the rods. Before 11 h the rods were too distinct from *S. aureus* to see polar bodies.

Fig. 10. Carbon-platinum shadowed 4 x 5 (magnification 10,000) prepared from 500 mesh at 31 K. This micrograph shows the fairly regular morphology of the cells. (X 10,000)

Fig. 11. Carbon-platinum shadowed 4 x 5 (magnification 10,000) prepared in cold electron. The arrows indicate areas which appeared to be forming at the poles of the rods. (X 10,000)

Fig. 12. Carbon-platinum shadowed 10 x 5 (magnification 10,000) prepared in cold electron. The arrows indicate areas which appeared to be forming at the poles of the rods and handles of cell-like structures (CMT). (X 10,000)

Fig. 13. Carbon-platinum shadowed 10 x 5 (magnification 10,000) prepared in cold electron. The arrow points out a structure as seen in this micrograph; the rods are of various lengths. Cell-like microstructure are indicated by CMT. (X 10,000)

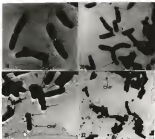
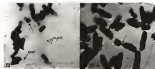


Fig. 11. Confocal-lensum obtained 70 h after driftless (M20) cultured in cell culture. The arrow indicates a free nucleus. The bodies were surrounded by solid and collinear microfilaments are indicated by GMR. (X 3,000)

Fig. 12. Confocal-lensum obtained 70 h after driftless (M20) cultured in cell culture. The arrow indicates a not end a nucleus formed by symmetrical division. (X 30,000)

Fig. 13. A light micrograph of a Gram stained preparation of *S. drifless* (M20) at 72 h in cell culture. The arrows indicate the darkly staining polar bodies which give the cells a beaded appearance. (X 3,000)



Stationary phase cells remained rigid for a longer period of time when cultured in soil extract as compared with YEM broth. In YEM broth the cells remained firm during exponential growth, but as the bacteria entered the stationary phase, the cells were collapsed. In soil extract the cells remained firm during stationary phase (after 24 h) and up to 36 h. The explanation for this is unknown at this time.

Long stained preparations of cells grown in soil extract showed beaded tails throughout the incubation period. Fig. 15 shows a light micrograph of a Gram stained preparation at 24 h. The arrows indicate the beak-like staining pole bodies which caused the cells to appear beaded. After 24 h in soil extract the beading was so pronounced that the tails could have been misinterpreted as outgrowths of cells. Further staining with crystal violet revealed that these were tails. For this reason it was difficult to resolve the actual cells. After 24 h there was little change in the Gram stained preparations. The tails had a tendency to become shorter and beading continued. After 36 h true cells were not detected with the light microscope, as had been the case with the electron microscope. It was difficult to resolve the actual cells from the beaded tails. The difference in tail length was not resolved by the light microscope.

Cells were prepared for thin sectioning and freeze-fracturing. The low frequency of occurrences of beaded tails is impossible to demonstrate beading at the poles of the tails.

Growth of *Brucella abortus* B40 in Clayer Beef Broth-Difco-Foster Talc medium as prepared had 50% dry weight of water. This appears to be the case. Most strains could not be concentrated greater than 30 when using lyophilized meat extracts since the dry material could not be completely dissolved.

Staphylococcus aureus was harvested from TSB broth at 12 h and transferred to root medium prepared at the following concentrations: 10 (100 µg/ml), 10 (200 µg/ml), and 10 (300 µg/ml). Fig. 24 shows that the optical density of cells cultured in 10 and 10 root medium decreased after the cells entered the stationary phase. The decrease in optical density was correlated with a decrease in cell mass, as seen in Fig. 25. Cells cultured in 10 concentrated root medium showed a slight decrease in optical density and cell mass during a 36 h incubation period.

Staphylococcus aureus was harvested from TSB broth at 12 h and transferred to 10 concentrated root medium. Fig. 26 shows the growth of *S. aureus* SAMP in this medium. The optical density of the culture began to decrease after 12 h. The total cell mass also began to decrease at this time. The generation time of *S. aureus* SAMP in 10 root medium was 4 h. As indicated in Table 1, the pH of the root medium increased slightly during growth of the bacteria.

The root medium contained some acid root exudates; it was thought that the acid root exudates were causing the decrease in optical density and dry weight. There are reports of acid root exudates (41,42) in the literature. It has been observed during this research that when acid exudates occurred at the top of the cover slip used in the Petri dish during rhizome incubation, a zone of inhibition of bacterial growth could be seen in the rhizosphere. The size of the zone of inhibition approximated to the size of the acid zone.

The final root medium was thought to contain phenolic compounds because of the dark brown color and the fact that phenolic compounds frequently occur in very high concentrations in plants. Lewis and Hinchell (43) described a technique using *Asotolnia polytrichosporium*

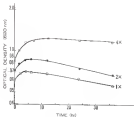


Fig. 14. Growth curves of *Rhodospirillum rubrum* in different concentrations of slurry (run constant Optical Density).

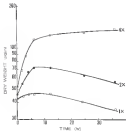


Fig. 11: Growth response of *Rhizobium meliloti* 300 to different concentration of clover root exudate (dry weight)

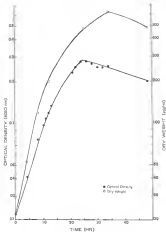


Fig. 20 Growth curve of *Bacillus subtilis* B2018 in concentrated citric acid solution

Table 4. Growth of *Blaschkea trifida* BGD cultured in 12-hour light periods

Time of Inoculation (hr)	Optimal Density x10 ⁶ ml ⁻¹	Growth Phase	pH of Medium
0	104	Immersion	7.2
1	106	Polysynponential	6.8
18	117	late Exponential	7.0
24	117	Stationary	7.2
72	130	Stationary	7.3

QPP) to elute phenolic compounds. The root exudates were collected through glass columns (II) in a 15 ml portion with vacuum, standard QPP. This treatment lowered the brown color of the root exudate.

Standard *Bradyrhizobium* BAC was harvested from TSB broth at 48 h and resuspended in PVP treated root exudates prepared at the following concentrations: 1.7 mg/ml, 3.3 mg/ml, 6.6 mg/ml, 13.3 mg/ml, and 6.6 mg/ml. PVP treated root exudate could be concentrated more than untreated root exudate.

The growth curves of *B. bradyrhizobium* BAC cultured in PVP treated root exudate is shown in Fig. 10. The more protection time of cells cultured in PVP treated root exudate was 4.5 h. The protection time was the same for the different concentrations of root exudate, but the total growth of the bacteria was substantially different. There was no decrease in optical density with cells cultured in PVP treated root exudate.

Agarose acid extract has been used as a component in growth media in the place of yeast extract. A non-sterilized agarose acid extract medium gave higher cell counts than 40% yeast extract medium (20% Clived acid extract was prepared by the method of Hayes and Rabenell (11). A medium was prepared which contained 20% clived acid extract (acidified) in root exudate (1.7 mg/ml). The addition of acid extract reduced the protection time of *B. bradyrhizobium* BAC from 4.5 h to 2.5 h (Fig. 11). The effect of different concentrations of acid extract in the medium was not tested.

Taxoids were prepared from cells incubated in PVP treated root exudate and concentrated to 10^8 cells/ml. Infection threads were counted after 5 days incubation. Infection threads were initiated in the time range of 30 to 42 h after inoculation when the taxoids were prepared

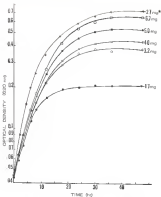


FIG. 10 Growth response of *Staphylococcus aureus* to different concentrations of PVP treated silver zinc nanowires. The 17 mg treatment (control) included 324 silver zinc nanowires.

from exponentially growing cells (through 12 h). Lanes prepared from stationary phase cells of 15 h and observed indicated infection through by 44 to 48 h.

The mean number of infection threads per swelling increased as the cells aged in non-swelling media (Table 7). After 7 days incubation in non-swelling, *S. trifolii* B&B produced 4 times as many infection threads per swelling as did cells incubated in non-swelling for 1 h. The environment of infectivity induced by non-swelling was more pronounced with larvae prepared from stationary phase cells than from exponentially growing cells.

Morphology of Staphylococcus trifolii. B&B cultured in serum and antibiotic-liquors were taken from several test swatches of larvae to determine if *S. trifolii* B&B passed through distinct morphological changes which could be related to capsule reproduction or constitute a life cycle.

The representative morphology of *S. trifolii* B&B cultured in non-swelling is shown in Fig. 20-22. The morphology of the 11 h incubation harvested from B&B broth was identical to that seen in Fig. 20. The larvae contained rods which were fairly uniform in morphology.

After 5 h in non-swelling there was an accumulation of both slime and capsule material which was not associated with the 11 h incubation. Slime was defined as the extracellular material which was loosely associated with cells. A capsule was defined as that material which completely surrounded and had physical contact with the bacterial cells. Fig. 23 shows cells which were subjected to a filtration matrix. The cellulose microfibrils radiated from the cells in bundles. Fig. 24 shows encapsulated cells. The capsule material lay on the cells

Table 1. Regression Results from Analysis (continued) for 1991-1992 and 1993-1994
 (continued from previous page)

1991-1992						
Panel	0 hr	1 hr	20 hr	24 hr	17 hr	1 hr
1	15	20	44	45	58	59
2	50	47	74	88	83	118
3	35	45	55	54	121	120
4	58	58	37	48	158	148
5	18	52	42	58	93	126
6	20	12	41	71	121	85

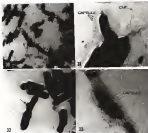
Notes: 0 hr = 0 hr; 1 hr = 1 hr; 20 hr = 20 hr; 24 hr = 24 hr; 17 hr = 17 hr; 1 hr = 1 hr.

Fig. 10. Carbon-platinum shadowed E & E. 100,000x. 50,000 collected in root shadow. This micrograph shows cells which had cellulose microfibrils (CMF) arranged in bundles. A fibrous material completely covers the background of the grid. (E 5,451)

Fig. 11. Carbon-platinum shadowed E & E. 100,000x. 50,000 collected in root shadow. A field of cells is surrounded by a fibrous capsule. (E 10,440)

Fig. 12. Carbon-platinum shadowed E & E. 100,000x. 50,000 collected in root shadow. The arrow indicates a bulge in the cell. (E 10,440)

Fig. 13. Carbon-platinum shadowed E & E. 100,000x. 50,000 collected in root shadow. The cells are completely surrounded by a fibrous capsule. (E 1,000)



appeared fibrous but was another in appearance away from the cells, cellulose microfibrils were more associated with cells (Fig. 14)

Scanning transmission showed cells were elongated in this view than in the LE & Scanning from TEM mode. There was an increased amount of extracellular material around the cells.

At 8 h in leaf mode LE was difficult to distinguish cellulose microfibrils from flagella. About 4 h in root mode there was a marked increase in the visibility of the cellulose as seen by scanning and shown under the phase microscope. Flagella may have been sheared from the cells and broken up due to the washing and sectioning procedure used in preparing cells for shadowing. It is thought that the structures seen in Fig. 20 were flagella. Not all cells were encapsulated (Fig. 21). However, as seen in Fig. 22, some cells were heavily encapsulated by a fibrous material. At 8 h & 12 h (Figs 23,24) was breaking down into as seen by the budding cells in Fig. 25. At 8 h the cells were too electron dense to see the polar bodies.

Scanning transmission at 4 h showed an intensely staining, extracellular material around clumps of cells. While the morphology of the cells was a fairly uniform size, there was a small number of special cells.

Figs 26-28 show cells at late exponential growth (12 h). At this time prior bodies were seen free in the culture. The cells were pleomorphic and the rods were of various lengths. Fig. 29 shows nonencapsulated cells associated with released prior bodies. As seen in Fig. 20, there was some with some cells. The rods seen in this micrograph are of different lengths. Fig. 30 shows an encapsulated cell and a released prior body.

Fig. 14. Carbon-platinum standard 12 h 3, dry/for 1958 cultured in root medium. Sides of various lengths are seen. PE indicates polar bodies which have been released into the medium. (X 5,715)

Fig. 15. Carbon-platinum standard 12 h 3, dry/for 1958 cultured in root medium. Sides of various lengths are shown associated with sides. PE indicates a released polar body. (X 5,195)

Fig. 16. Carbon-platinum standard 12 h 3, dry/for 1958 cultured in root medium. An unpenetrated cell is shown with a released polar body (PE). (X 10,200)

Fig. 17. Carbon-platinum standard 12 h 3, dry/for 1958 cultured in root medium showing sides of various lengths associated with sides. (X 4,244)

Fig. 18. Carbon-platinum standard 12 h 3, dry/for 1958 cultured in root medium showing sides of various lengths associated with sides. (X 5,715)



From stained preparations at 12 h about an increased amount of extracellular material. The cells could barely be seen, but appeared as rounded rods when visible.

In 14 h (Fig. 37 and 38) the cells were still rigid and not collapsed. As seen in Fig. 37 and 38, the filum surrounded the cells. Short, rounded rods with ends of this filum but no curre were observed. From stained preparations of 14 h cells appeared the same as the 12 h cells.

Cells at 44 h are seen in Fig. 39 and 40. At this time a number of curre were observed in the medium. Fig. 39 shows a curre, and next to it a cell which appears to be in budding. A phagocytic cell is seen in Fig. 40. This appears to be a binucleated filament. A pleomorphic cell such as this one is rare occurrence. At 44 h the cells were less rigid and polar bodies could be seen in some cells (Fig. 40). From stained preparations at this time about rounded rods. The budding was so pronounced that a regular pattern of stained and unstained areas was seen. This budding with the cells (rod) appear as analogs of curre. Positive staining with crystal violet revealed that these were curre.

In 72 h most cells were collapsed (Fig. 41 and 42). At this time polar bodies could be distinctly seen within the rods. The rods were of different lengths. Curre were not apparent at this time. As seen in Fig. 41, filum was associated with some cells. From stained preparations about cells with very swollen and banded. The swollen cells were rounded only.

Endothelial-Plant Interactions—STORAGE. unfertilized root hairs, as seen in Fig. 43, occurred in remarkably great frequency

Fig. 10. *Carbonyplaxium shastense* 18 h. 8. 0x1000 1000
cultured in root medium. The unlabeled active polystyrene + carbon
+ polymorphs and its area seen in the center. (X 1,700)

Fig. 11. *Carbonyplaxium shastense* 18 h. 8. 0x1000 1000
cultured in root medium. A long branched filament is seen in
the center of the micrograph. 75 indicates the polar bodies
in the bacteria. (X 1,700)

Fig. 12. *Carbonyplaxium shastense* 70 h. 8. 0x1000 1000
cultured in root medium showing a line of collapsed cells which
are visible along. The cells are associated with slime and 75
indicates the polar bodies. (X 1,700)

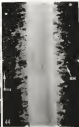
Fig. 13. *Carbonyplaxium shastense* 70 h. 8. 0x1000 1000
cultured in root medium showing a line of cells which are
visible along. 75 indicates polar bodies inside the cells and
where which are released from the medium. (X 1,700)



Fig. 43. Axially grown sleeve with undeformed root
(wire 080) (X 100).

Fig. 44. Short, axially deformed root hairs (20) on
sleeve associated with 2. 100/010. RAGS harvested from TES
trunk at 21 h. The bacteria are concentrated in the outer
region and are indicated by "line" (X 100).

Fig. 45. Long, axially deformed root hairs on sleeve
associated with 2. 100/010. RAGS harvested from TES trunk at
17 h. The bacteria are concentrated in the subapical and
are indicated by "line" (X 100).



usually following a reaction called closure). Fig. 44 shows deformed root hairs on a flower inoculated with *P. trifolii* B32. The incidence fluctuates in the rhizosphere and appeared as large clumps. The intensity or degree of root hair deformation could be correlated with the degree of rhizobia inoculated into the rhizosphere. When the inoculum contained greater than 10^8 rhizobia, the root hairs were markedly deformed and situated in approximately one half the length of uninoculated root hairs (as seen in Fig. 44). These curled root hairs were less than 2.0 mm long, with lower cell counts (less than 10^3 rhizobia), root hairs were moderately curled and as long as, or longer than, uninoculated root hairs (Fig. 45). These moderately curled root hairs were greater than 2.0 mm long. Deformation through old tissue in long root hairs, but high infection through tissue (more than 10^8 infection through per rhizosphere field with the 100 objective) were restricted to areas along the root where root hair growth was arrested.

The characteristic curled root hair tip, which is referred to as a shepherd's crook, is seen in Fig. 46. Root infection through elongated in the shepherd's crook, as seen in Fig. 47. When tissue was prepared from 100 hour infected roots, approximately 10% of the infection through was observed to originate from unfurled root hair tips. When tissue was prepared from roots infected in three root nodules, the incidence of infection through infection in unfurled root hairs was approximately 10%. When the infected root hair did not have a shepherd's crook, a right retroviral bacterium flag could be seen at the infection through angle.

Early infected infection through connected only slightly with

Fig. 46. Tightly curled root hair with Golayland's vesicle, 600 \times as shown associated with *B. brachyloca*. 84.50 harvested from YEM broth at 72 h. (X 1,450)

Fig. 47. Cellulose thread (17) in a root hair with a sharp bend's neck (80) formation. The swelling was associated with *B. brachyloca*. 84.50 harvested from YEM broth at 72 h. (X 1,400)



46



47

the cytoplasm of the host cells (Fig. 40). In the isolation chamber used with this, all bacteria were light refractile and distinct. The host cells without nuclei is observed at the tip of the growing filament (Fig. 41).

Shigella boydii B20 grown in association with clostridia could be found either unaggregated or aggregated (Fig. 38-39) when *S. boydii* B20 in the clostridia microcapsules with capsules of various sizes. As seen in Fig. 38 and 39, a capsule could contain more than one horizontal cell. The isolation of several horizontal cells in single capsules was observed only when *S. boydii* B20 was grown in association with clostridia in clostridia isolation medium (Fig. 38-42). Serial sections of these capsules which contained more than one cell, showed that the fibrillar material completely surrounded the bacteria. Bacteria could be observed embedded in an amorphous material attached to the host cells surface as seen in Fig. 38. Fig. 39 shows capsules which appear to be the capsules but attached capsules. *Shigella boydii* B20 cells in the microcapsules were pleomorphic only when isolated in saline, otherwise the cells had a fairly uniform rod morphology.

Shigella boydii B20 was observed attached to host cells in a polar arrangement as seen in Fig. 38. As pointed out in the Classification Review (see page 10), the relationship for polar attachment is unknown. When the chemical structure of capsules differs for horizontal attachment, it known, specific microchemical tests can be used in studying attachment with the electron microscope. The slide section seen in Fig. 39 shows fibrils radiating from the cell. This material stained positively for polysaccharide with the periodic acid-silver hematoxylin stain (44).

The light microscope has been invaluable in studying such isolated agents in the synthesis of host cells and bacterial attachment.

Fig. 48. Root hair penetrating on infection thread (100 \times) which is being fed toward toward the root cap by the root hair nucleus (P). [X 400]

Fig. 49. Higher magnification of Fig. 48 showing the infection thread (100 \times) and the root hair nucleus. [X 1,000]

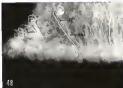


Fig. 13. A thin section of unrecrystallized bacteria within the clastic rhinophores. This section shows an unrecrystallized bacterium and a diaphanous which contained the bacterium. (X 11,700)

Fig. 14. A thin section of an unrecrystallized bacterium in the clastic rhinophores. (X 10,800)

Fig. 15. A thin section of unrecrystallized and partially recrystallized bacteria in the clastic rhinophores. (X 14,700)

Fig. 16. A thin section of unrecrystallized and unrecrystallized bacteria in the clastic rhinophores contains a root hair. (X 10,700)

Fig. 14. A thin section of an unrecrystallized bacterium embedded in an amorphous material attached to the root hair wall. (X 10,700)

Fig. 15. A thin section of bacteria which contained more than one bacterium. The capsule has a segmented appearance. (X 14,700)



Fig. 26. A root hair with *E. trifolius* 8420 attached in a polar orientation. The arrow indicates an attached bacterium. (X 1,150)

Fig. 27. An electron micrograph of a thin section of a polarly attached *E. trifolius* 8420 cell. (X 15,000)



In addition, the light microscope has been used to study the growth of the infection thread through the root hair. However, the point of entry, and thus the physical mechanism, cannot be resolved with the light microscope. In this study, seedlings were prepared for electron microscopy in order to resolve such issues and determine if there was an invagination. The technique of critical point-drying was used so the root hairs could be mounted in an osmium.

Root hairs having the shoot's growth at the infection thread origin were serially sectioned, and in every case, the root hairs still wall was invaginated. There were no breaks in the root hairy wall wall at the point of entry, and the root hairy wall wall was continuous with the wall of the infection thread.

Fig. 10 is a schematic illustration of a sectioned root hair based on a serial section sequence from which Fig. 11-14 were selected. The invagination was seen before, through, and past the pore (Fig. 10, 11, and 12, respectively). Bacteria were seen within the pore and in the infection thread. This infection thread may have been easily initiated before the fixation, as it had not progressed far into the root hair, and the nucleus is seen in close association with the tip of the infection thread.

As shown in this serial section sequence, the infection thread wall at the point of invagination is difficult to see (indicated by arrows in Fig. 11-14). However, the infection thread walls away from the point of invagination are clearly distinguishable. This may reflect a physical and/or chemical alteration of the cell wall structure at the invagination origin, where the specific bacteria-plant interaction resulted in the initiation of an infection thread.

Fig. 33. A diagrammatic illustration of a partial molting run being started by infection thread (IT), molting (M), and the initiation of molting (M) (arrows).

Fig. 34. A vertical thin section before the invagination showing the infection thread which contained bacteria (B). The arrow indicates the region of the post hair wall where the invagination process has begun. (21, 128)

Fig. 35. A vertical thin section through the middle of the invagination showing the infection thread well advanced at the pole, bacteria (B) within the infection thread, and the post hair molting. (21, 128)

Fig. 36. A vertical thin section past the pole; the arrows point out where the wall of the pole is grown by the cells. (21, 128)



54



55



56

Serial sections through a root hair with an infection thread which did not originate in the originally infected rhizoplast's neck are shown in Fig. 43-48. Fig. 43 is a diagrammatic illustration of the root hair based on serial sections from which the sequence in Fig. 43-48 was selected. The root hair was slightly curved. The infection thread originated midway on the root hair and branched during growth through the root hair. Each branch grew into the root of the root hair. The root hair sections are positioned next to the branch point at the time of fixation. A line of bacteria was attached to the root hair at the origin of the infection thread. The sectioning began at the Elor (arrow) and continued through the root hair. The plasma wall of the attached filar was ground (Fig. 43), and then bacteria were revealed inside (Fig. 44). Several sections were cut through the filar before the root hair wall was reached (Fig. 45). The arrows in Fig. 45 indicate the interface between the root hair wall and the filar. The filar had a segmented appearance (Fig. 45 and 46). An infection continued progressively through the root hair, as disintegration of the root hair wall became apparent (Fig. 46). Continuing through the area where the infection thread originated revealed a pore filled with and surrounded by the filar (Fig. 47). The wall of the root hair was continuous with the infection thread wall (Fig. 47-48). The filar descended in size past the middle of the pore (Fig. 49) and ended as the back wall of the pore was ground by the knife (Fig. 49). Bacteria were seen within the infection thread (Fig. 49-50).

The section of the root hair (Fig. 50) was positioned by the infection thread (from Fig. 45-50). The sections do though to have provided the infection thread access to the root hair layer in the root cortex, and then to have migrated to this point before fixation occurred.

Fig. 41. A diagrammatic illustration of a serial unopened root hair with an infection thread which did not originate in a rhizopod's neck. The infection thread (IT) originated midway on the root hair and branched below the surface (B). A piece of bacteria (B) was attached to the root hair at the origin of the infection thread. Excreting hyphae of the filar (indicated by the top arrow) and root hairs through the root hair.

Fig. 42. The slime wall (arrow) of the attached filar is covered by the hyphae in this serial thin section. Unmycelinated *D. desulfurans* were seen in the rhizosphere. (X 9,170)

Fig. 43. A serial thin section in which the filar is unopened and the bacteria are covered hyphae. The arrow indicates the slime surrounding the filar. (X 9,170)

Fig. 44. A serial thin section in which the root hair wall is grazed by the hyphae. The arrow indicates the hyphae between the root hair and the attached filar. (X 9,170)



62



63



64



65

Fig. 46. A serial thin section showing where the root wall will be beginning to diverge into [arrows]. The attached disc has a sigmoidal appearance. (X 11,500)

Fig. 47. The root hair wall is diverging to form the sub-ridge throat in this serial thin section. The plant wall will [arrows] be continuous with the wall of the sub-ridge throat. Bacteria are seen within the disc and the sub-ridge throat. (X 9,000)

Fig. 48. A serial thin section past the middle of the divergence. The plant wall wall is indicated by the arrows. (X 11,500)

Fig. 49. A serial thin section in which the back wall [arrows] of the divergence is passed by the leafy, the attached disc has ended at this point. (X 11,400)



64

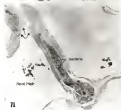
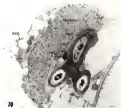


66



Fig. 30. A thin section of the root hair nucleus which is partitioned near to the infection thread. The infection thread is composed of the distal layer, an outer fibrillar layer (OL) and an inner amorphous layer (IL). Fungus (F) are seen within the infection thread. The nucleus had numerous nuclear pores (NP). The cytoplasm surrounding the infection thread contained sugar ribosides (R) and rough endoplasmic reticulum (RER). Vesicles (V) were seen fusing with the root hair cell wall and the infection thread. (X 10,000)

Fig. 31. A thin section showing the branch point (indicated by arrows) of the infection thread (IT). One branch of the infection thread extends from the root hair cell into the root cell layer in the root cortex. There is no alteration in the continuity of the infection thread walls at the plant plasmalemma. (X 35,000)



This would be in accordance with observations by Fahrenius (19) and McGraw (20) that the root hair nucleus provides the growing infection thread into the base of the root hair cell. Fig. 36 shows numerous nuclear pores in the nuclear envelope. Punctules undoubtedly produced by the nucleus were seen leading with the root hair wall and with the infection thread wall.

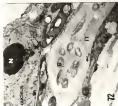
The infection thread, as seen in Fig. 35, was composed of two distinct layers, an outer layer and an inner amorphous layer, surrounding the bacteria. The inner amorphous layer was visible in the electron lens and would be missing in thinned sections. The outer layer of the infection thread and the plant cell wall appeared similar in appearance. Both walls showed features for polysaccharide with the periodic spiral-shaped branches (21). However, the inner layer did not stain. If this layer contained polysaccharide, it was not sensitive to periodic acid oxidation.

Fig. 34 shows the branch point of the infection thread (indicated by arrow) with one branch invading into the underlying cell. The process of the infection thread opening from one cell into another in the cortex appeared to be a repetition of the invagination process which occurred at the original site of infection. There was no disruption in the continuity of the infection thread, and the wall of the infection thread and the plasmalemma were continuous.

Fig. 37 and 38 show infection threads adjacent to nuclei. In each instance there was an accumulation of finely staining, diffuse material between the nucleolus and the nuclear envelope. This may represent transfer of ribonucleoprotein from the nucleolus to the cytoplasm. It has been thought by several workers (22,23) that there is a direct

Fig. 72 A thin section of an infection thread (IT) adjacent to the plant cell nucleus. The nucleus contained a prominent nucleolus (N) which had a diffuse, darkly staining material associated with it (indicated arrow). The bacteria within the infection thread are indicated by B. (X 12,000)

Fig. 73 A thin section of an infection thread (IT) which grew from the base of the root hair. The root hair nucleus was adjacent to the root hair tip. The nucleolus (N) had a diffuse, darkly staining material associated with it (indicated arrow). The bacteria within the infection thread are indicated by B. (X 12,000)



backbone) immediately beneath the stem (Fig. 14) and the growing infection spread as the nucleus produced the growing tip of the infection thread into the base of the root hair cell.

Figs. 12 and 13 were taken from separate serial section sequences. In each case the nucleolus was a prominent nuclear structure. Fig. 12 was taken from the serial section sequence after the largest part of the nucleolus was sectioned. In this case the nucleolus appeared smaller in this section.

DISCUSSION

A study of the ultrastructure of *S. irishii* B20 was undertaken to determine if the organism passed sequentially through distinct morphological forms that could constitute a life cycle as proposed by several early Rhizobium workers.

Rhizobium irishii B20 had a mean generation time of 3 h when cultured in YEM broth. The cells were the same surface in size and shape during sub-exponential growth. In contrast, no cells grown in soil extract and root exudate, the cells were morphologically not shaped, no root were observed using the electron microscope. As the cells entered stationary phase, there was a tendency for the bacteria to become rounded. Asymmetrical cell division during growth resulted in cells of various lengths. Binary fission was the only mode of cell division observed.

In soil extract *S. irishii* B20 had a mean generation time of 3.3 h. The concentration of soil extract did not affect the generation time of the bacteria, but did affect the total cell yield. *Rhizobium irishii* B20 was not observed to go through any complex life cycle when cultured in soil extract. Binary fission was the only mode of cell division observed. The surface area of the bacteria increased from YEM broth to soil extract of various lengths through asymmetrical division. Cells were produced during growth in soil extract. Short and long cells were noticeable at the poles of the cells at 3 h during exponential growth but were not observed later in the culture until 16 h.

One striking feature of the life cycle observed by various early workers was that the juvenile or mature was the infective form of *Monoxenus*. Table 3 shows that after 36 h, bacteria prepared from soil extracts began to decrease in infectivity. Such was not observed from in the medium until after 36 h, at which time the infectivity was significantly reduced.

In test medium B, *desulfos. B30* had a mean generation time of + h (and 25% variation) in the medium caused a decrease in cell density and dry weight measurements as the cells entered the stationary phase. There was no decrease in optical density with cells cultured in test medium treated with 70% to remove the acid fast bacteria. The concentration of test medium did not affect the growth rate of the bacteria but did affect the total cell yield. The addition of eleven acid bacteria to test medium caused a decrease in the generation time. The reason for this decrease in generation time is unknown.

As with *desulfos* and cell counts, no regular life cycle was observed in test medium and binary fission was the only mode of cell division observed. Cells cultured in test medium did produce spores, but these small cells constituted less than 1% of the total population of cells. Cells cultured in test medium became heavily overproduced and were associated with clots. This was unique to cells cultured in test medium and was not seen when the cells were cultured in *desulfos* broth or soil extracts.

The bacteria were pleomorphic and were subject to constant cell divisions. However, the pleomorphic form did not constitute a life cycle but rather was a response to growth conditions such as nutrient limitation. In *desulfos* broth, soil extracts, and test medium the bacteria were predominantly bacillary. Under the light microscope beaded cells

would be seen in all three media. The banding apparently was attributed to the accumulation of PEG and the darkly staining polar bodies. It is believed that these banded rods correspond to the "goodlings" observed by early workers, and the polar bodies correspond to the previously described "goodies." If a cell lysed and released the polar bodies into the medium, it would appear, under the light microscope, as if a "swirly cell" had released "swimmers." It is concluded that the life cycle of the mite, as proposed by some early Heliothis workers, was an erroneous interpretation of events prepared for the light microscope.

Definitively studies showed that the morphology of the invasion would not be correlated with infectivity. Invasion prepared from stationary phase cells in YEM broth was significantly more infective than was invasion prepared from exponentially growing cells in the same medium. Host hair marking ability and bacterial observation did not account for the differences in infectivity.

According to the "polyphasicism" theory of Ajlouni and Johnson (41), the extracellular polysaccharide of infective *TM* cells plays an important role in specificity and infection. With *P. fluorescens* B30, stationary phase cells produced more extracellular polysaccharide than did exponentially growing cells. However, in preparing the invasion, cells were centrifuged from YEM broth and resuspended in sterile PBS. For this extracellular polysaccharide to influence infection, it would have to be active at low concentrations. This is not unreasonable as plant hormones are active at concentrations as low as 10^{-12} M for indole-3-acetic acid (28). It is noted at this time, that specific function, if any, the extracellular polysaccharide has in the infection process:

The seedling was inoculated with bacteria when the stationary phase slide inoculations were prepared. Stationary phase cells may have survived this initial starvation period, before plant root exudates accumulated, better than an inoculum prepared from cells harvested at mid-exponential growth from TSB broth. As indicated in Table 1, the number of bacteria in the inoculum did affect the same number of infection threads formed. The difference in the number of infection threads formed from stationary phase cells and exponentially growing cells would indicate that the population of exponentially growing cells would have to be reduced by an order of magnitude of three to account for the difference in infectivity.

Cells cultured in root extract did not change their infectivity while growing exponentially, however cells in stationary phase produced fewer infection threads per seedling. Inspection of the rhizosphere of seedlings inoculated with stationary phase cells revealed no obvious reasons why these cells would be less effective than exponentially growing cells.

The opposite effect was seen for cells cultured in root exudate. Inocula prepared from stationary phase cells produced significantly more infection threads than did inocula prepared from exponentially growing cells. This enhancement of infectivity may have been due to either the growth phase of the cells or the decreased time of exposure of the bacteria to root exudate. These two possibilities could not be differentiated during the experiment. Light microscopic examination of the rhizosphere of seedlings inoculated with root exudate cultured cells showed an increased number of bacterial filae attached to root hairs. The incidence of infection thread initiation is substantiated just

larger was detected even that after 100-200 days post infection. A sample prepared from stationary phase B. subtilis 168 released its endospores had more attached bacterial flora and infectious spores in unfertilized host tissue than did seedlings inoculated with nonsporulating growing cells from host nodules.

Selectivity of an infection could not be correlated with the morphology of the cells. The current data of the rhizobium prepared as a means of explaining how the bacterial cell penetrated the plant cell wall. Beijerinck (1) demonstrated that Rhizobium did not hydrolyze cellulose. The question arises as to how bacteria which could not degrade the plant cell wall could infect the plant cells. Philip (55) confirmed that the rhizobia did not hydrolyze cellulose or pectin when cultured in media containing these substrates.

The large scale production of hydrolytic enzymes would be detrimental to the establishment of the symbiosis as the rhizobia would have the potential to be pathogenic. The infection of the legume by the rhizobia must proceed in such a manner that the physiology of the plant be affected as little as possible. A major disruption of the host cell physiology results in abortion of the infection process (56).

Microautoradiographic evidence presented by this research shows that the bacteria enter the root hair by a process of invagination. The bacteria restrict the growth of the plant cell wall so that the root hair grows both later basally. In this way, the bacteria enter the root hair through a bacterium-induced, plant synthesized infection thread which results from the invagination process. The bacteria travel unopposed while inside the root hair.

Infection threads in seedlings inoculated for seven days with

remained and the pores were open. At this time it is unknown if the pores remain open for a longer period of time. The pores are not directly exposed to the rhizosphere but are either restricted by the sheath's cross (Fig. 10-11) or plugged with a film of mucous (Fig. 11-12). In this way, entry into the infection channel could be limited to those bacteria trapped in the sheath's cross or in the bacteria completing the film. This may explain the independent occurrence of infection of roots from one strain of *Aschersonia* from one isolate.

The majority of infected root hairs have the tightly coiled root hairs (Fig. 10) but infection will occasionally occur in a relatively uncoiled root hair. It is believed that the affected bacterial film on the tightly coiled root hairs (Fig. 11) causes the same damage as the tightly coiled root hairs (Fig. 10). Investigating and understanding the biochemical interactions of the plant and bacteria to a threshold level which is required for initiation of infection.

Seedlings inoculated with root isolate cultured bacteria showed an increased number of infection channels originating from uninfected gain hairs. These infection channels originated from attached bacterial films. It is proposed that isolating the bacteria in closed root isolate increased the susceptibility of the bacteria which enabled the bacteria to infect a greater number of root hairs. In addition, these uncoiled bacteria may have stimulation infection to occur in less time than roots cultured in YES or soil extracts.

Future studies on infection should concentrate on determining what role the rhizosphere and bacterial polysaccharides play in the infection process and the specific biochemical interactions which allow infection to take place and result in the degeneration of the plant root cell.

3. Olson, C. V., and E. C. Allen. 1966. Response of the potato plant to inoculation with rhizobia, with special reference to morphological development of the nodule. *Sci. Soc.* 181: 125-142.
4. Amarger, S., M. Heron, and E. Blackburn. 1967. Polymorphisme microcellulaire de *Rhizobium meliloti*. *Ann. J. Microbiol.* 21: 75-81.
5. Beijerinck, W. J. 1906. Die bacterien der pflanzennodulierung. *Bot. Tij.* 44: 709-804.
6. Boyly, R. F., and R. S. Buchanan. 1959. Is the change through which the nodule organism (*Rhizobium*) passes under repeated conditions? *J. Agric. Sci.* 93: 343-347.
7. Elmer, R. A. 1942. Growth and survival of *Rhizobium* in soil. *J. Gen. Microbiol.* 7: 115-161.
8. Elmer, R. A. 1955. Some characteristics of *Rhizobium* species from tropical legumes. *J. Gen. Microbiol.* 10: 33-48.
9. Elmer, R. A., and C. R. F. Hale. 1951. The production of nodules in *Rhizobium* sp. *J. Gen. Microbiol.* 5: 542-555.
10. Galloway, G. E., and R. L. Schmidt. 1955. Immunological detection of *Rhizobium japonicum* in soils. *Soil Sci.* 118: 279-285.
11. Galloway, G. E., and R. L. Schmidt. 1954. Lysing: a possible basis for specificity in the *Rhizobium-legume* nodule synthesis. *Science* 105: 365-375.
12. Galloway, G. E., and R. L. Schmidt. 1956. Immunofluorescent stain test of *Rhizobium japonicum*: possible site of attachment for lysing binding. *J. Bacteriol.* 121: 1189-1195.
13. Henshaw, F. B. 1959. Penicillin response in inoculated and naturally formed clover nodules. *Plant Soil* 10: 149-158.
14. Jones, G. B. 1963. The nodality of legume root diffusions caused rhizobia and other bacteria. *Plant Soil* 15: 155-163.
15. Jones, G. B. 1968. Production of growth substances by clover nodule bacteria. *Nature* 221: 751-754.

10. Gray, A. L., L. R. Greenough, and G. A. Williamson. 1973. Physicochemical characteristics of cellulose hemicellulose of lichen modules and their chemical significance with Rhizobium. Arch. Microbiol. 37:31-36.
11. Gray, A. L., and G. A. Williamson. 1972. Three hemicelluloses of cellulose hemicellulose and their physicochemical character. Arch. Microbiol. 37:143-148.
12. Hart, P. J. 1971. Imaging electron microscopy of plant cells. J. Exp. Bot. 22:113-121.
13. Hart, P. J. 1974. The lichen system, p. 211-425. In A. S. Hitchcock (ed.), The Biology of Lichens. Plenum Press, New York.
14. Hart, P. J., and P. S. Hynes. 1974. The lichen rhizomorphs. Arch. Microbiol. 37:241-249.
15. Hynes, P. S., and P. S. Hynes. 1975. Cytoplasmic streaming and lichen as a mechanism of cytoplasmic streaming in the Rhizomorphs. Arch. Microbiol. 37:143-148.
16. Hynes, P. S., and P. S. Hynes. 1975. Formation of cellulose hemicellulose by lichen rhizomorphs and their role in lichen development. Arch. Microbiol. 37:143-148.
17. Hynes, P. S., and P. S. Hynes. 1975. Rhizomorphs with particular reference to relationships with host plants. Arch. Microbiol. 37:143-148.
18. Hynes, P. S. 1974. Competition in Rhizomorph species. J. Botanical. 37:129-130.
19. Hynes, P. S., and J. Hynes. 1974. Ecological studies of lichen rhizomorphs. Arch. Microbiol. 37:143-148.
20. Hynes, P. S. 1974. Growth and extracellular polysaccharide production by Rhizomorph species in defined media. J. Botanical. 37:129-130.
21. Hynes, P. S. 1975. The isolation of lichen host cells by culture techniques studied by a simple glass slide technique. J. Bot. Microbiol. 37:143-148.
22. Hynes, P. S. 1975. Studies on the lichen rhizomorph system. Arch. Microbiol. 37:143-148.
23. Hart, P. J. 1974. Studies on the life cycle of lichen rhizomorphs. Arch. Microbiol. 37:143-148.

18. Gibson, T. 1912. Observations on *P. ruber* (Kütz.) J. Agric. Sci. 26: 75-81.
19. Graham, P. B. 1961. Extracellular polysaccharides of the genus *Shewanella*. *Adv. in Microbiol., J. Microbiol., Ser. 1*: 285-314.
20. Graham, P. B., L. J. Baker, E. T. Long, and L. J. L. Davidson. 1961. Spore Formation and host resistance in *Shewanella*. *J. Bacteriol.* 75: 1232-1234.
21. Harsh, E. 1964. Über den Einfluss der Keimkonzentration auf die Virulenz von *Legionella* und *Legionellaceae*. *Zeitschr. Bakteriell. Fortschritt Abt. 11* 121: 343-344.
22. Kaper, G. 1951. Composition of extracellular polysaccharides of *Shewanella bryellii*. *Adv. in Microbiol., J. Microbiol., Ser. 1*: 457-461.
23. Kijalki, J. 1944. Electron microscopic studies on the helical thread developing in the root hair of *Erpichlamydia* L. Infected with *Shewanella bryellii*. *J. Gen. Microbiol.* 12: 393-403.
24. Kijalki, J. K. 1938. Studies on the root hair "necrotic factor" of *Shewanella*. *Acta Soc. Sci. 111*: 33-342.
25. Kijalki, J. K., and J. B. Fineman. 1939. Bacteriological studies of the root-necrosis bacteria. II. Test of neutralizing capacity of the same species. *Proc. Univ. (for B.S.B.)* 42: 241.
26. Kijalki, J. K. 1948. Resistance of L-D-glutamic acid to *Shewanella* genus bacteria. *Acta Soc. Sci.* 101: 466.
27. Kijalki, J. K., and J. B. Fineman. 1939. Extracellular polysaccharides of *Shewanella*. *J. Gen. Microbiol.* 11: 411-424.
28. Loomis, F., and F. E. Chomsky. 1932. Isolation of cytoplasmic and extract for growth of *Shewanella* spp. *Zeitschr. Bakteriell. Fortschritt Abt. 117*: 244-247.
29. Loomis, F. T. 1938. Effect of isoleucine on rate of elongation of root hairs of *Agrostis alba* L. *Physiol. Plant.* 1: 133-45.
30. Loomis, F. T. 1940. Survival of *Shewanella* isolates in soil cultures. *Science* 110: 612-613.
31. Loomis, F. T., and J. B. Fineman. 1935. Identification of the *Shewanella* strains in pea root necrosis using genetic methods. *J. Gen. Microbiol.* 4: 343-358.
32. Loomis, F. T., and F. E. Chomsky. 1932. The application of leucine-¹⁴C to the study of root plant/bacteria interactions selectively using *Erpichlamydia* systems. *Cell Biol. Biophys.* 4: 175-221.

42. Smith, I. H. 1938. Plant infections and the life cycle of *Phytophthora*. *J. Bacteriol.* 35: 511-527.
43. H. E. and R. E. Bennett. 1949. Infection thread formation as a basis of substrate specificity in Rhizobium-leguminous flower associations. *Can. J. Microbiol.* 15: 1153-1156.
44. Lillish, T. T., and E. W. Khan. 1948. Evidence concerning the role of polygalacturonase in invasion of root halves of leguminous plants by *Rhizobium* spp. *Can. J. Microbiol.* 14: 817-823.
45. Klotzmann, E. G., E. G. Schmidt, and E. C. Cox. 1954. Evidence for double infection with *Rhizobium* nodulin. *Soil Sci.* 128: 374-379.
46. Ljunggren, R. 1945. Mechanism and pattern of *Rhizobium* invasion into leguminous root halves. *Physiol. Plant Supp.* 3: 46 p.
47. Ljunggren, R., and E. Petersen. 1941. The role of polygalacturonase in root infection by nodulin bacteria. *J. Gen. Microbiol.* 14: 621-628.
48. Leitch, P., and R. B. Smith. 1918. Life cycles of the bacterium. *J. Agr. Res.* 1: 673-720.
49. Lewis, F. G., and E. Bennett. 1951. Plant phenolic compounds and the invasion of plant enzymes. *Phytochem.* 1: 423-430.
50. Buchanan, A. R., and R. Alexander. 1951. Comparison of nodulating and non-nodulating strains of *Rhizobium* nodulin. *Plant Soil* 33: 110-118.
51. Klotzmann, E. G., and E. C. Cox. 1955. Evidence against involvement of plant enzymes in the invasion of root halves by *Rhizobium* nodulin. *Can. J. Microbiol.* 13: 943-945.
52. Bennett, R. E., and R. E. Gledhill. 1953. Cell surface hydrophobicity and the colonization of certain bacteria of leguminous. *Arch. Microbiol.* 31: 25-30.
53. Bennett, R. E., R. E. Gledhill, and R. E. A. Ruppel. 1953. The colonization of certain root-nodule bacteria on interfaces including liquid root-half surfaces. *J. Gen. Microbiol.* 11: 128-136.
54. McFar, E. 1952. Infection by *Root Nodules* in relation to the symbiogenesis of the host's cell walls. *Proc. R. Soc. London Ser. B* 385: 309-320.
55. Hesse, J. H. 1948. Bacteria's breakdown of protein and total-nitrogen of the infection of *Rhizobium* in *Physalis*. *Plant Soil* 30: 117-124.
56. Bapat, G., P. Bapat, and R. Bennett. 1955. Microstructure of infection and "nodulin analysis" on infection by *Rhizobium*. 1st Australian Legume Conference, March 18-21, 1955, Brisbane, Australia.

58. Kuylenstierna, G., E. Rönner, and B. Wiklund. 1975. Production of cellulosic oligosaccharides by *Microthrix*. *Appl. Microbiol.* 30: 120-124.
59. Rönner, E. B. 1977. The influence of the fungus in microbe-plant symbiosis: A comparative study of host characteristics and fungal-plant link. *Ann. Garbholms Palace Bot.* 34:109-131.
60. Rönner, E. B. 1979. Some observations on root hair infection by mycorrhizal bacteria. *J. Exp. Bot.* 30:299-302.
61. Rönner, E., E. B. J. Bengtsson, P. J. Hest, and B. B. Wiklund. 1979. Effect of low temperature germination on infection of clover root hairs by *Microthrix*. *Plant Soil* 55:227-239.
62. Peters, R. J., and R. Alexander. 1966. Effect of fungus inoculation on the root nodule bacteria. *Soil Biol.* 100:392-397.
63. Phillips, R. A., and J. C. Toney. 1970. Cellulose production by *Microthrix japonica*. *Physiol. Plant.* 19:1611-1661.
64. Rydberg-Kjær, J. 1947. Preliminary studies of ultrastructural (ultrastructural) localization in root tip cells. *J. Microscop. Cytol.* 10:442-450.
65. Rydberg, R., B. Rönner, and P. Hest. 1975. Binding of *Microthrix japonica* to cultured soybean root nodules: morphological evidence. *Plant Soil* 44:201-210.
66. Rydberg, R. B. 1945. The use of host elements as an electron-transporter in electron microscopy. *J. Cell Biol.* 15:299-313.
67. Smiley, A. B. 1961. Interactions between plant roots and soil microorganisms. *Ann. Rev. Microbiol.* 15:343-348.
68. Smiley, A. B. 1966. Plant root nodules and their influence upon soil microorganisms. p. 149-184. In R. F. Brady, R. G. Snyder, and J. Ecology of soilborne plant pathogens. John Wiley, London.
69. Sjöberg, E., and E. Fehrmann. 1963. Microscopic observations on the effect of indole-3-acetic acid upon root hairs of *Trifolium repens* Lp. *Lundskva-Bogskol. Arb.* 28:234-244.
70. Sjöberg, E., and E. Fehrmann. 1961. An electron microscope study of root hair infection by *Microthrix*. *J. Gen. Microbiol.* 23:415-427.
71. Strong, R. C., and R. V. B. Clements. 1974. Bacterioplant symbiosis in microbial communities: Population dynamics and the role of the plant in the symbiotic association. *Microbiol. Rev.* 38:149-159.

11. Schmidt, R. 1940. Die Bedeutung der abendlichen Verwitterung von Alpiden-Graniten und ihre Bedeutung aufbauen. *Flora* 114:1-11.
12. Schmidt, R. L., E. S. Schmidt, and R. S. Schmidt. 1961. Fluorescence-microscopy approach to study of Alpidia (L. 1911). *J. Microscop.* 15:189-199.
13. Schmidt, R. 1942. Contributions to the history of Alpidia 1. Alpidia Alpidia is a synthetic compound name. *Bot. Soc.* 14:189-191.
14. Schmidt, R., and J. Sch. 1971. Evidence supporting the theory of specific induction of protein-degrading enzymes in roots for overwintering in Alpidia-lycopodium associations. *Plant Soil* 19:475-486.
15. Schmidt, R., and J. Sch. 1972. Characterization of the substances causing inhibition of root growth of *Profilium repens* when associated with Alpidia-lycopodium. *J. Soc. Microscop.* 77:841-842.
16. Stone, E. 1934. Detailed analysis of overwintering, 1934 polyp overwintering from various Alpidia species. *Geophytica Soc.* 12:15-16.
17. Stone, A. S. 1945. A low viscosity spray resin embedding medium for electron microscopy. *J. Microscop.* Soc. 19:12-13.
18. Stone, E. 1961. How the Alpidia was characterized by the root and overwintering and overwintering. *Flora* 1:1-10. (See also: Lycopodium Roth Microscop. Soc. 11:141-142).
19. Thompson, J. A. 1966. Inhibition of root growth by an antibiotic from Lycopodium and roots. *Science* 153:413-415.
20. Thompson, E. C., and E. Thompson. 1968. The life cycle of the Alpidia-lycopodium Alpidia Alpidia (L. 1911) in soil, and its response to infection of the host plant. *Plant Soil* 19: 421-432.
21. Trichak, R. J. 1971. Interactions between Alpidia and the host-lycopodium. *Flora* 1:1-10. (See also: 1972).
22. van Ruyven, J. H. J. H. 1972. Free-root seedlings and their effect upon overwintering Alpidia. *Wissenschaften Lycopodium*, Wageningen 17-18, Netherlands: 90 p.
23. Vincent, J. H., S. Heston, and R. J. Heston. 1961. Some features of the fine structure and chemical composition of Alpidia-lycopodium. *J. Soc. Microscop.* 16:151-152.
24. Van, P. T., and J. H. Heston. 1945. Root overwintering in the host plant "wintering host" of Alpidia spp. *Ann. J. Biol. Sci.* 12: 423-425.

84. Drenth-Hansen, L. R., T. R. 1971. Chemical composition of *Parasitasterias* of Rhaphidion and *Aporrhasterion*. J. 599, Microbiol. 48 234-242

GEOGRAPHICAL NOTES

Devlin Ann Lois Spill was born April 19, 1944, in Marianna, Texas. She was graduated from Lakeland High School in Lakeland, Florida, June 1964. In June 1965 she received the Associate of Arts degree from Santa Fe Junior College, Deltona, Florida. In June 1971 she received the Bachelor of Science degree with a major in microbiology from the University of Florida, Deltona, Florida. She began her graduate studies at the University of Florida in September 1971. She is a member of the American Society for Microbiology, the Postgraduate Branch of the American Society for Microbiology, and the Society of Sigma Xi. She is currently a candidate for the Ph.D. degree in the Department of Microbiology, University of Florida.

She has one child, Jean-Marie Ellen Spill.

I certify that I have read this study and that in my opinion it conforms to acceptable standards of scholarly presentation and is fully adequate, in scope and quality, as a dissertation for the degree of Master of Philosophy.


David R. Hull
Associate Professor of Cell Microbiology

I certify that I have read this study and that in my opinion it conforms to acceptable standards of scholarly presentation and is fully adequate, in scope and quality, as a dissertation for the degree of Master of Philosophy.


Henry C. Johnson
Professor of Microbiology and Cell Science

I certify that I have read this study and that in my opinion it conforms to acceptable standards of scholarly presentation and is fully adequate, in scope and quality, as a dissertation for the degree of Master of Philosophy.


Arnold E. Kluge
Professor of Microbiology and Cell Science

I certify that I have read this study and that in my opinion it conforms to acceptable standards of scholarly presentation and is fully adequate, in scope and quality, as a dissertation for the degree of Master of Philosophy.


L. O. Kohn
Associate Professor of Microbiology
and Cell Science

I certify that I have read this study and that in my opinion it embodies an exceptional standard of scholarly presentation and is fully adequate, in scope and quality, as a dissertation for the degree of Master of Philosophy.



Edward P. Bernie
Associate Professor of Manuscriptology
and Coll. Relations

This dissertation was submitted to the Graduate Faculty of the College of Arts and Sciences and to the Graduate Council, and was accepted as partial fulfillment of the requirements for the degree of Master of Philosophy.

August, 1974

Dean, College of Arts and Sciences

Dean, Graduate School